ARMY RESEARCH LABORATORY

Trade-Offs in Performance Enhancement of Solid-Propellant (SP) Electrothermal-Chemical Guns

Phuong Tran
Gloria Wren

ARL-TR-692 February 1995

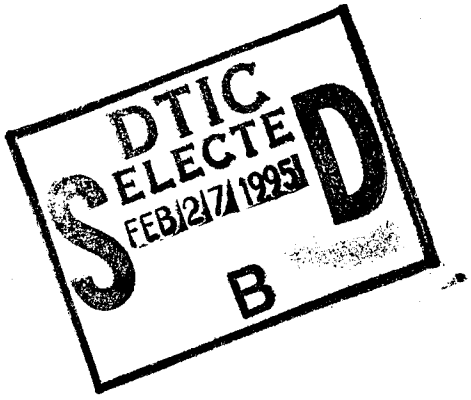

NOTICES

Destroy this report when it is no longer needed. DO NOT return it to the originator.

Additional copies of this report may be obtained from the National Technical Information Service, U.S. Department of Commerce, 5285 Port Royal Road, Springfield, VA 22161.

The findings of this report are not to be construed as an official Department of the Army position, unless so designated by other authorized documents.

The use of trade names or manufacturers' names in this report does not constitute endorsement of any commercial product.

REPORT DOCUMENTATION PAGE

Form Approved
OMB No. 0704-0188

1. AGENCY USE ONLY *(Leave blank)*	2. REPORT DATE	3. REPORT TYPE AND DATES COVERED
	February 1995	Final, January 1993–December 1993

4. TITLE AND SUBTITLE

Trade-Offs in Performance Enhancement of Solid-Propellant Electrothermal-Chemical Guns

5. FUNDING NUMBERS

PR: 1L162618A1FL

6. AUTHOR(S)

Phuong Tran and Gloria Wren

7. PERFORMING ORGANIZATION NAME(S) AND ADDRESS(ES)

U.S. Army Research Laboratory
ATTN: AMSRL-WT-PA
Aberdeen Proving Ground, MD 21005-5066

8. PERFORMING ORGANIZATION REPORT NUMBER

9. SPONSORING / MONITORING AGENCY NAME(S) AND ADDRESS(ES)

U.S. Army Research Laboratory
ATTN: AMSRL-OP-AP-L
Aberdeen Proving Ground, MD 21005-5066

10. SPONSORING / MONITORING AGENCY REPORT NUMBER

ARL-TR-692

11. SUPPLEMENTARY NOTES

12a. DISTRIBUTION / AVAILABILITY STATEMENT

Approved for public release; distribution is unlimited.

12b. DISTRIBUTION CODE

13. ABSTRACT *(Maximum 200 words)*

The design of a solid-propellant electrothermal-chemical (SPETC) gun includes a number of choices for propellant and electrical energy. The trade-offs inherent in the choices affect the maximum pressure and muzzle velocity as well as pulse power size. Three questions of interest are addressed theoretically in this paper: (1) Is the optimal web determined from a conventional, optimal, solid-propellant (SP) calculation altered by the addition of electrical energy? (2) Are there trade-offs between power and energy, and, hence, pulse power size, to attain equivalent performance? (3) Can grain progressivity and post-maximum-pressure (post-Pmax) plasma energy injection work together to optimize gun performance at higher loading densities?

14. SUBJECT TERMS

electrothermal, interior ballistics, solid propellants

15. NUMBER OF PAGES

53

16. PRICE CODE

17. SECURITY CLASSIFICATION OF REPORT	18. SECURITY CLASSIFICATION OF THIS PAGE	19. SECURITY CLASSIFICATION OF ABSTRACT	20. LIMITATION OF ABSTRACT
UNCLASSIFIED	UNCLASSIFIED	UNCLASSIFIED	UL

INTENTIONALLY LEFT BLANK.

ACKNOWLEDGMENTS

The authors would like to thank the reviewers, Dr. Terence Coffee and Mr. Gary Katulka. Mr. William Oberle, Mr. Fred Robbins, and Dr. Kevin White's comments and suggestions are appreciated. In addition, Dr. Arpad Juhasz originated the questions addressed in this report.

INTENTIONALLY LEFT BLANK.

TABLE OF CONTENTS

		Page
	ACKNOWLEDGMENTS	iii
	LIST OF FIGURES	vii
	LIST OF TABLES	ix
1.	INTRODUCTION	1
2.	OPTIMAL WEB INVESTIGATION	3
2.1	Optimal Web for the Conventional SP Gun	3
2.2	Optimal Web for the SP Electrothermal-Chemical Gun	5
2.2.1	Post-Pmax Plasma Injection	5
2.2.2	Pre- and Post-Pmax Plasma Injection	8
2.3	PFN Design	15
2.3.1	PFN for Post-Pmax Plasma Injection	15
2.3.2	PFN for Pre- and Post-Pmax Plasma Injection	17
2.3.3	Pros and Cons for Post-Pmax and Pre- and Post-Pmax Plasma Injections	17
3.	ELECTRICAL ENERGY AND POWER TRADE-OFFS	19
4.	PROGRESSIVITY	31
4.1	SPETCIB Model	31
4.2	IBHVG2 Model	32
4.2.1	Test 1	32
4.2.2	Test 2	34
4.3	Comparison Between the Gun Performance From the IBHVG2 Calculation and From the CONPRESS Calculation	38
5.	CONCLUSIONS	39
6.	REFERENCES	41
	DISTRIBUTION LIST	43

INTENTIONALLY LEFT BLANK.

LIST OF FIGURES

Figure		Page
1.	Schematic of an electrothermal-chemical gun	2
2.	Pressure vs. time (M30, post-Pmax)	7
3.	Power vs. time (M30, JA2, post-Pmax)	7
4.	Pressure vs. time (JA2, post-Pmax)	7
5.	Pressure vs. time (using SPETCIB with various timemax)	13
6.	Pressure vs. time (M30, pre- and post-Pmax)	13
7.	Power vs. time (M30, JA2, pre- and post-Pmax)	14
8.	Pressure vs. time (JA2, pre- and post-Pmax)	14
9.	PFN diagram for post-Pmax plasma injection	16
10.	Designed pulse power shape for post-Pmax injection	16
11.	PFN circuit diagram for pre- and post-Pmax plasma injection	18
12.	Designed pulse power shape for pre- and post-Pmax plasma injection	18
13.	Muzzle velocity vs. power (loading density = 1.0 g/cm^3)	21
14.	Muzzle velocity vs. power (loading density = 1.1 g/cm^3)	22
15.	Muzzle velocity vs. power (loading density = 1.2 g/cm^3)	23
16.	Muzzle velocity vs. power (loading density = 1.3 g/cm^3)	24
17.	Muzzle velocity vs. electrical energy and power (loading density = 1.0 g/cm^3)	25
18.	Muzzle velocity vs. electrical energy and power (loading density = 1.1 g/cm^3)	26
19.	Muzzle velocity vs. electrical energy and power (loading density = 1.2 g/cm^3)	27
20.	Muzzle velocity vs. electrical energy and power (loading density = 1.3 g/cm^3)	28
21.	Muzzle velocity vs. power with various loading densities	29
22.	Muzzle velocity vs. propellant mass with various power and EE = 1.0 MJ	30

Figure		Page
23.	Muzzle velocity vs. propellant mass with various power and EE = 2.0 MJ	30
24.	Muzzle velocity vs. propellant mass with various power and EE = 3.0 MJ	31
25.	Pressure vs. time with various perforations (SPETCIB model, 7.0 kg JA2)	33
26.	Pressure vs. time (M30, 1 perf)	35
27.	Pressure vs. time (M30, 37 perf)	36
28.	Muzzle velocity vs. loading density from the IBHVG2 and the CONPRESS calculations (M30 Propellant, 37 perf, EE = 3 MJ)	38

LIST OF TABLES

Table		Page
1.	Gun Parameters Used in Simulation	4
2.	Optimal Performance of Conventional SP Gun With JA2 and M30 Propellants	4
3.	Summary of SPETC Gun Performance With Post-Pmax Plasma Injection, 5 MJ, 3 GW, and M30 7-Perf Propellant	5
4.	Summary of SPETC Gun Performance With Post-Pmax Plasma Injection, 5 MJ, 3 GW, and JA2 7-Perf Propellant	6
5.	M30 Propellant, Gun Performance With Varying Timemax (Propellant Mass = 7.1 kg)	8
6.	M30 Propellant, Option 1, Gun Performance With Different Propellant Mass	8
7.	M30 Propellant, Option 2, Gun Performance With Different Propellant Mass	9
8.	M30 Propellant, Option 3, Gun Performance With Different Propellant Mass	10
9.	JA2 Propellant, Gun Performance With Varying Timemax (Propellant Mass = 6.9 kg)	10
10.	JA2, Option 1, Gun Performance With Different Propellant Mass	11
11.	JA2, Option 2, Gun Performance With Different Propellant Mass	11
12.	JA2, Option 3, Gun Performance With Different Propellant Mass	12
13.	Optimal Performances	15
14.	Test Matrix for Energy and Power Trade-Offs Investigation	20
15.	The Gun Performances With Varying SP Perforation and Propellant Mass (3 MJ, 1.6 GW)	32
16.	Summary of Study on the Effect of Electrical Energy Level on Propellant Burnt With 500 MPa Pmax	37

INTENTIONALLY LEFT BLANK.

1. INTRODUCTION

The electrothermal-chemical (ETC) gun has five main components: (1) prime power supply and intermediate storage batteries; (2) pulse forming network (PFN) and switching; (3) plasma cartridge; (4) combustion chamber; and (5) barrel and projectile as shown in Figure 1.

The ETC gun concept uses high-energy, high-loading density propellant and a plasma energy source to increase muzzle velocity and control gun performance. An electrical energy source is used to generate plasma inside the plasma cartridge. This plasma energy is then injected into the combustion chamber through a nozzle and functions as an igniter. It may augment muzzle velocity as well, through the addition of energy, and is intended to control the interior ballistics (IB) process. The solid-propellant electrothermal chemical (SPETC) gun combustion chamber is filled with a solid-propellant (SP) charge. This gun concept is a conventional gun with additional plasma energy. The design concept embodies the advantages of plasma energy with the advantages of SP in terms of repeatability. In addition, there exists a body of charge design methodology from SP application. Thus, the SPETC gun has the potential to increase performance at minimal risk.

We know that the web size or grain progressivity and loading density (ratio of propellant mass to chamber volume) are key factors in determining gun performance. In addition, in the ETC gun, electrical energy influences not only maximum pressure but the propellant gas generation rate as well, due to increased pressure in the combustion chamber. The objective of this report is to determine the trade-offs between progressivity, loading density, and electrical energy to optimize gun performance. Gun performance is measured in terms of muzzle velocity and maximum chamber pressure. From a practical point of view, trade-offs may not only affect choices of propellant and loading density but may influence pulse power supply as well.

Theoretically, electrical energy in the form of plasma can be injected into the combustion chamber after the combustion chamber reaches its desired maximum pressure or can be injected at the beginning and during the IB process. In this report, the first scenario is called post-maximum pressure (post-Pmax) plasma injection and the second is called pre- and post-maximum-pressure (pre- and post-Pmax) plasma injection. Both methods of adding energy to the system are investigated in this report.

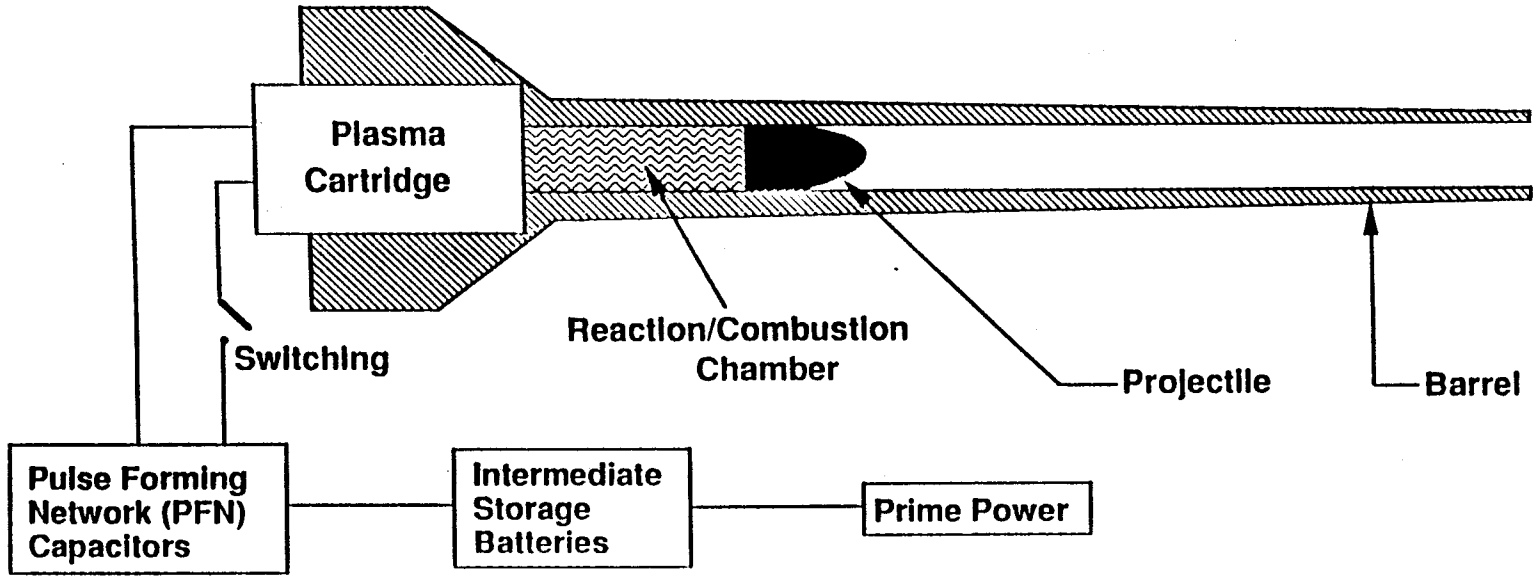

Figure 1. Schematic of an electrothermal-chemical gun.

There are three parts to this paper:

(1) The gun performance with different sizes of propellant web at varying loading density is studied for both post-Pmax plasma injection and pre- and post-Pmax plasma injection. A comparison between the performances of these injection schemes is made, and the pros and cons of each case will be discussed. In addition, a PFN was designed for the required pulse power shape and is presented.

(2) The trade-offs between total electrical energy and the power delivered to the plasma capillary are determined parametrically. The study shows how fast a given amount of electrical energy is delivered (power) to the plasma capillary, providing a significant contribution to the gun performance.

(3) An investigation of the effect of grain progressivity and electrical energy level to optimize the gun performance at high loading density is presented.

Two IB models are used in this study: a standard lumped parameter model, IBHVG2 (Fickie and Anderson 1987), and the SPETCIB (Morrison, Wren, and Oberle 1991, 1992) model. The SPETCIB code was chosen because of its ability to optimize based on the variation of the input electrical energy. With this model, unlike IBHVG2, we can define the shape of the desired pressure profile and determine the corresponding input energy profile. The optimal shape of the electrical energy profile, which is required to maintain the pressure at its maximum, is also included in this model. The formulations and assumptions of the code are described in the references. In addition, P2SIM (Princeton Combustion Research Laboratories, Inc. 1992), a new pulse power simulation, was also used to design the desired PFN.

2. OPTIMAL WEB INVESTIGATION

2.1 Optimal Web for the Conventional SP Gun. In order to investigate the optimal web of the conventional SP gun, an IBHVG2 simulation with varying loading density was performed for both propellants M30 and JA2. The gun parameters which are used in the simulation for this study are based on a 105-mm ETC gun fired by the Soreq Nuclear Research Center (SNRC), Israel (Juhasz at al. 1992a, 1992b), and are listed in Table 1.

Table 1. Gun Parameters Used in Simulation

Parameter	Value
Bore diameter	105 mm
Chamber volume	7,130 cm^3
Projectile mass	4.4 kg
Projectile travel	924 cm
Maximum breech pressure	550 MPa
Propellants	M30, JA2 (7 perf)
Propellant mass	varying

The optimal performances for the gun parameters described in Table 1, using the IBHVG2 simulation, are 1997 m/s muzzle velocity for M30 propellant at loading density 0.995 g/cm^3; and 2,040 m/s muzzle velocity for JA2 propellant at loading density 0.967 g/cm^3. The results of propellant mass and grain geometry for each propellant are shown in Table 2.

Table 2. Optimal Performance of Conventional SP Gun With JA2 and M30 Propellants

	M30	JA2
Muzzle Velocity	1,997 m/s	2,040 m/s
Propellant Mass	7.1 kg	6.9 kg
Propellant Size (7 Perf)		
Optimal Web	0.1331 cm	0.0799 cm
Diameter (D)	0.7066 cm	0.4696 cm
Length (L)	1.254 cm	1.52 cm
Perf. Diameter (DP)	0.058 cm	0.05 cm
L/D	2.1567	3.2368
D/DP	12.1833	9.392

2.2 Optimal Web for the SP Electrothermal-Chemical Gun. The parameters which give the optimal performance using the IBHVG2 simulation were applied to the SPETCIB simulation. The results from both the IBHVG2 and the SPETCIB simulations were equivalent. Thus, the parameters will be used as the baseline. For this study, a square power pulse of 3 GW for 1.67 ms duration (5 MJ) is assumed to be supplied into the plasma capillary and the performances with two types of plasma injections are investigated: (1) post-Pmax plasma injection and (2) pre- and post-Pmax plasma injection.

2.2.1 Post-Pmax Plasma Injection. In this type of plasma injection, in order to maintain the maximum chamber pressure, plasma energy is delivered into the combustion chamber after the breech pressure reaches its maximum value. Since the expectation is that more propellant will be burnt due to the added electrical energy, the range of studied charge masses starts from the optimal propellant mass for the conventional SP gun (7.1 kg for M30 and 6.9 kg for JA2) up to the amount that leaves some unburnt propellant in the combustion chamber.

The summaries of the optimal gun performances from SPETCIB simulation for M30 and JA2 propellants with different propellant masses are shown in Tables 3 and 4 respectively.

Table 3. Summary of SPETC Gun Performance With Post-Pmax Plasma Injection, 5 MJ, 3 GW, and M30 7-Perf Propellant

Prop. Mass (kg)	Web (cm)	Muzzle Velocity (m/s)	Prop. Burnt (%)	Diff. to the Optimal SP only (%)
7.1	0.1331	2,133	100	+ 6.81 baseline
7.2	0.1364	2,135	100	+ 6.91
7.3	0.1398	2,137	100	+ 7.01
7.4	0.1433	2,139	100	+ 7.11 optimal
7.5	0.1469	2,138	100	+ 7.06
7.6	0.1506	2,138	100	+ 7.06
7.7	0.1543	2,136	100	+ 6.96
7.8	0.1582	2,134	99.9	+ 6.86

Table 4. Summary of SPETC Gun Performance With Post-Pmax Plasma Injection, 5 MJ, 3 GW, and JA2 7-Perf Propellant

Prop. Mass (kg)	Web (cm)	Muzzle Velocity (m/s)	Prop. Burnt (%)	Diff. to the Optimal SP Only (%)
6.9	0.0799	2,165	100	+ 6.13 baseline
7.0	0.0820	2,167	100	+ 6.23
7.1	0.0842	2,168	100	+ 6.27
7.2	0.0864	2,169	100	+ 6.32 optimal
7.3	0.0887	2,168	100	+ 6.27
7.4	0.0911	2,166	99.9	+ 6.18

From Tables 3 and 4, we can see that the optimal loading density in an SPETC gun is slightly larger than that in a conventional SP gun (1.03 g/cm^3 compared to 0.99 g/cm^3 for M30 and 1.01 g/cm^3 compared to 0.96 g/cm^3 for JA2). Even though the plasma energy does affect the amount of propellant consumed, the optimal loading density is not quite as high as expected. The reason is that in order to meet the limitation of maximum breech pressure, the size of the propellant web must be adjusted to slow down the total energy release. This web size is larger than the optimal web size for a conventional SP gun (0.1433 cm compared to 0.1331 cm for M30 and 0.0864 cm compared to 0.0799 cm for JA2). However, as shown in Tables 3 and 4, using 5 MJ of electrical energy and conventional propellants, there is no significant improvement in muzzle velocity of the SPETC gun at the optimal loading density compared to the muzzle velocity at the baseline loading density (0.30% for M30 propellant and 0.19% difference in muzzle velocity for JA2 propellant). Thus, performance is felt to be equivalent for both cases under the given constraints.

The breech pressure profiles of the SP gun and of the SPETC gun with post-Pmax plasma injection and the pulse power history for the optimal cases (M30 and JA2) are plotted in Figures 2–4. The optimal pulse power shapes for both M30 and JA2 propellant are the same; and the muzzle velocity with JA2 propellant is higher than M30 by 1.4%.

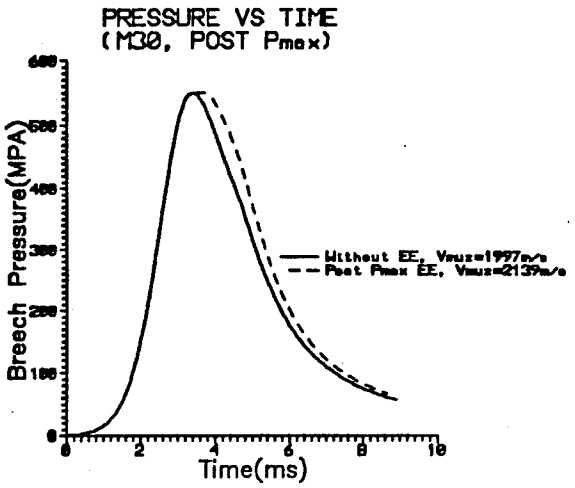

Figure 2. Pressure vs. time (M30, post-Pmax).

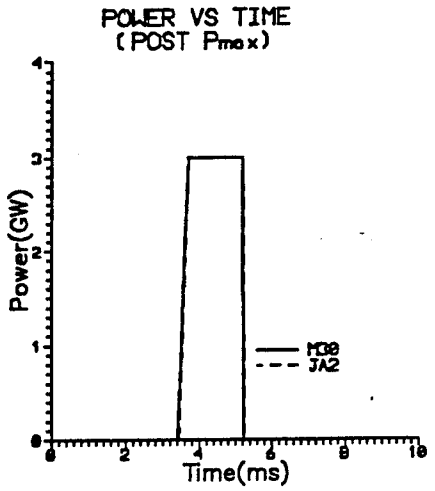

Figure 3. Power vs. time (M30, JA2, post-Pmax).

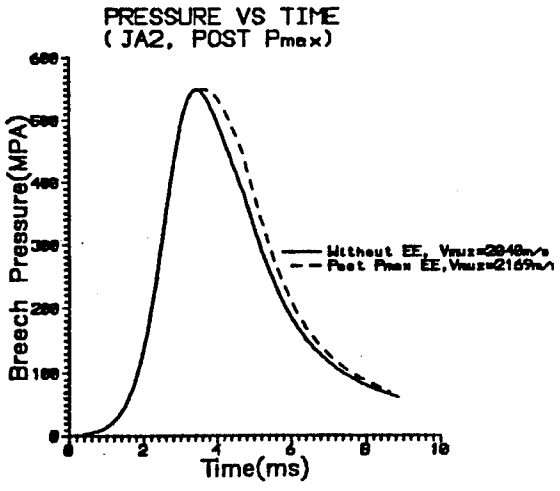

Figure 4. Pressure vs. time (JA2, post-Pmax).

2.2.2 Pre- and Post-Pmax Plasma Injection. The desired pressure profile should rise rapidly to maximum pressure and remain there as long as possible for maximum performance. There are three options in calculating the pressure and the corresponding electrical energy profiles for pre- and post-Pmax injection in the SPETCIB model: (1) Option 1: The model determines both the pressure and electrical power profiles, (2) Option 2: The user defines pressure rise rate based on the desired maximum pressure and time of maximum pressure (timemax), and (3) Option 3: The user defines the pressure rise rate during the early portion of the IB process, and the model will determine the pressure and power profiles required to approach Pmax later in the cycle. All three of these options were tested in order to find the optimal gun performance.

At first, we vary the input timemax and record the performance for each option. Then, the percentage of propellant consumed is observed, and the loaded propellant mass is adjusted in order to obtain the optimal case. The results are shown in Tables 5–8 for M30 and Tables 9–12 for JA2.

Table 5. M30 Propellant, Gun Performance With Varying Timemax (Propellant Mass = 7.1 kg)

Timemax (ms)	Option 1		Option 2		Option 3	
	Optimal Web (cm)	Muzzle Velocity (m/s)	Optimal Web (cm)	Muzzle Velocity (m/s)	Optimal Web (cm)	Muzzle Velocity (m/s)
0.5	0.1442	2,117	0.2100	1,786	0.1676	2,030
3.0	0.1442	2,117	0.1419	2,119	0.1390	2,127
4.5	0.1442	2,117	0.1380	2,126	0.1371	2,129

Table 6. M30 Propellant, Option 1, Gun Performance With Different Propellant Mass

Prop. Mass (kg)	Optimal Web (cm)	Muzzle Velocity (m/s)	Prop. Burnt (%)
7.0	0.1411	2,116	100
7.1	0.1442	2,117	100
7.2	0.1477	2,116	100
7.3	0.1517	2,113	99.9

Table 7. M30 Propellant, Option 2, Gun Performance With Different Propellant Mass

Timemax (ms)	Prop. Mass (kg)	Optimal Web (cm)	Muzzle Velocity (m/s)	Prop. Burnt (%)
0.5	5.5	0.1305	1,974	100
	5.6	0.1335	1,977	99.9
	6.5	0.1556	1,945	97.7
	7.1	0.2100	1,786	77.3
3.0	7.0	0.1391	2,117	100
	7.1	0.1419	2,120	100
	7.2	0.1455	2,119	100
	7.3	0.1489	2,119	100
4.5	7.1	0.1380	2,126	100
	7.2	0.1416	2,128	100
	7.3	0.1450	2,129	100
	7.4	0.1485	2,128	100
	7.5	0.1520	2,126	100

Table 8. M30 Propellant, Option 3, Gun Performance With Different Propellant Mass

Timemax (ms)	Prop Mass (kg)	Optimal Web (cm)	Muzzle Velocity (m/s)	Prop. Burnt (%)
0.5	6.2	0.1340	2,061	100
	6.3	0.1375	2,062	100
	6.4	0.1410	2,061	100
	6.5	0.1445	2,059	99.9
	6.9	0.1595	2,044	98.8
	7.1	0.1676	2,030	97.9
3.0	7.0	0.1361	2,124	100
	7.1	0.1390	2,127	100
	7.2	0.1426	2,127	100
	7.3	0.1461	2,127	100
4.5	7.1	0.1371	2,129	100
	7.2	0.1405	2,130	100
	7.3	0.1436	2,132	100
	7.5	0.1510	2,130	100

Table 9. JA2 Propellant, Gun Performance With Varying Timemax (Propellant Mass = 6.9 kg)

Timemax (ms)	Option 1		Option 2		Option 3	
	Optimal Web (cm)	Muzzle Velocity (m/s)	Optimal Web (cm)	Muzzle Velocity (m/s)	Optimal Web (cm)	Muzzle Velocity (m/s)
0.5	0.0874	2,143	0.1264	1,796	0.1009	2,052
3.0	0.0874	2,143	0.0859	2,148	0.0839	2,157
4.5	0.0874	2,143	0.0830	2,158	0.0824	2,161

Table 10. JA2, Option 1, Gun Performance With Different Propellant Mass

Prop. Mass (kg)	Optimal Web (cm)	Muzzle Velocity (m/s)	Prop. Burnt (%)	Comments
6.9	0.0874	2,143	99.9	Option 1 is independent to timemax.
6.8	0.0849	2,145	100	
6.7	0.0829	2,146	before exit 0.289 ms	
6.5	0.0799	2,138	before exit 0.797 ms	

Table 11. JA2, Option 2, Gun Performance With Different Propellant Mass

Timemax (ms)	Prop. Mass (kg)	Optimal web (cm)	Muzzle Velocity (m/s)	Prop. Burnt (%)
0.5	6.9	0.1264	1,796	74.9
	5.6	0.0829	2,003	99.3
	5.3	0.0749	2,014	100
	5.2	0.0730	2,010	100
3.0	6.9	0.0859	2,148	100
	6.8	0.0834	2,148	100
	6.7	0.0814	2,147	100
4.5	6.8	0.0810	2,156	100
	6.9	0.0830	2,158	100
	7.0	0.0854	2,158	100
	7.1	0.0875	2,158	100
	7.2	0.0895	2,156	99.9

Table 12. JA2, Option 3, Gun Performance With Different Propellant Mass

Timemax (ms)	Prop. Mass (kg)	Optimal Web (cm)	Muzzle Velocity (m/s)	Prop. Burnt (%)
0.5	6.9	0.1009	2,052	96.9
	6.2	0.0839	2,091	99.8
	6.0	0.0794	2,093	100
	5.9	0.0774	2,091	100
	5.8	0.0754	2,089	100
3.0	6.7	0.0799	2,154	100
	6.9	0.0839	2,157	100
	7.0	0.0864	2,155	100
	7.1	0.0884	2,155	99.9
4.5	6.8	0.0804	2,159	100
	6.9	0.0824	2,161	100
	7.0	0.0849	2,161	100
	7.1	0.0869	2,161	100

From these tables, some conclusions can be drawn:

- Option 3, the combination of user and code-defined pressure profile, finds the best performance.

- The longer time to reach maximum pressure (larger timemax), combined with a smaller web, gives better performance (shown in Figure 5).

- The SPETC gun performance using conventional propellants is not significantly improved by increasing the loading density beyond the optimal propellant mass of the conventional case. The total amount of propellant consumed to give the best performance is not as much as expected using the propellants specified. In addition, there is no difference in the performance of the two plasma injection methods studied. It is noted that these results may change with deterred grains which aid in the progressivity of the propellant.

The pressure history and power profiles of the optimal cases for M30 and JA2 with post- and pre-Pmax plasma injections are plotted in Figures 6–8.

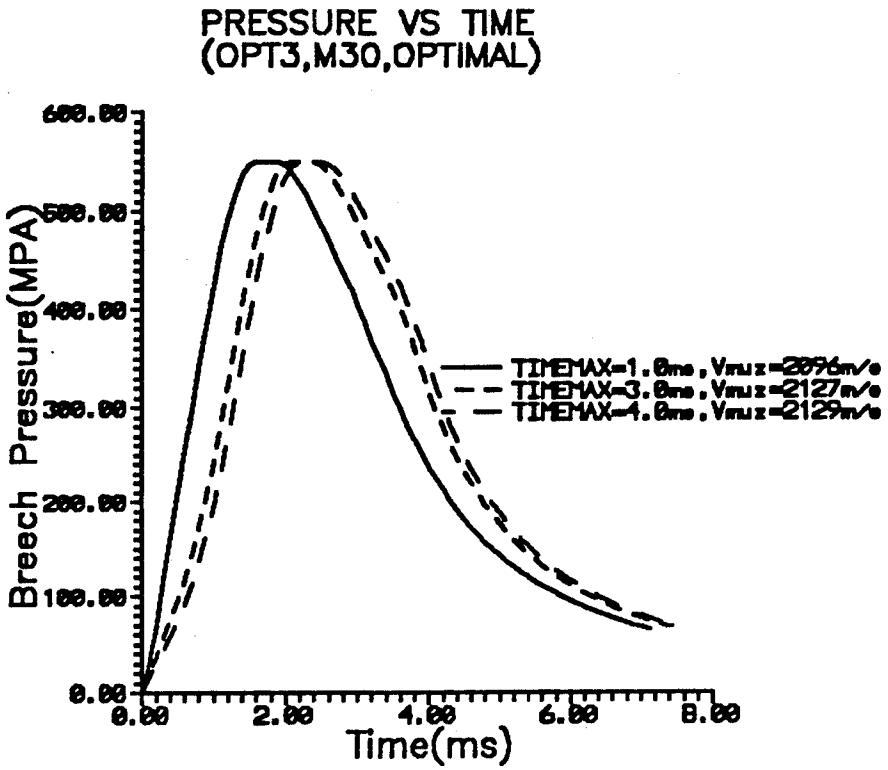

Figure 5. Pressure vs. time using SPETCIB with various timemax.

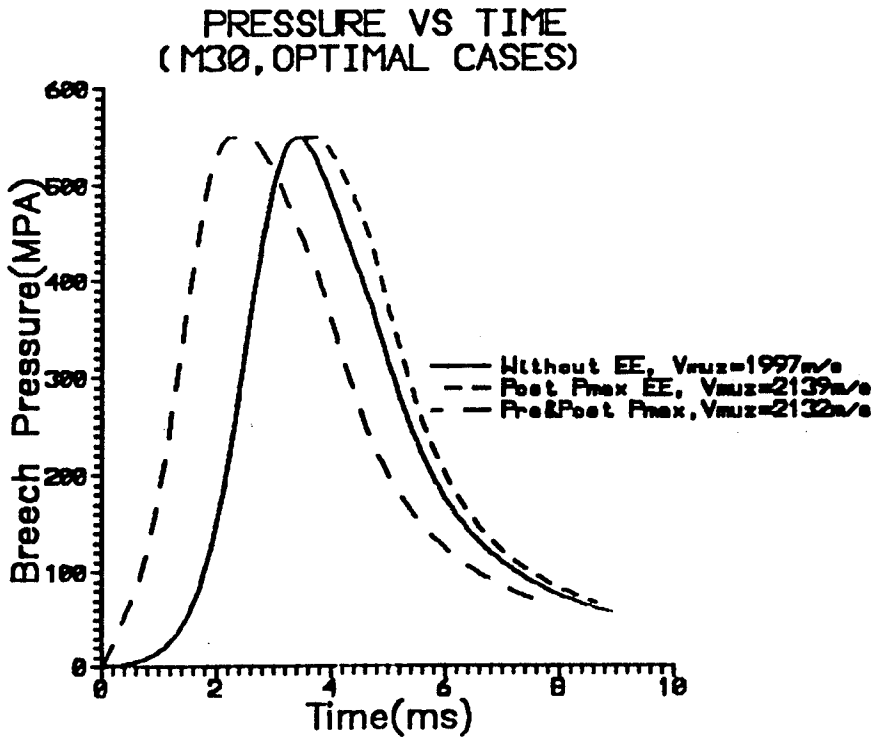

Figure 6. Pressure vs. time (M30, pre- and post-Pmax).

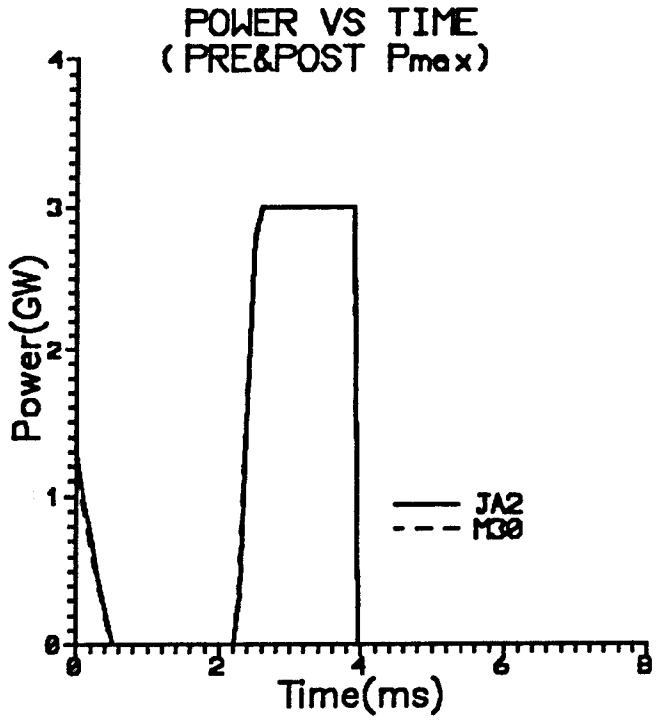

Figure 7. Power vs. time (M30, JA2, pre- and post-Pmax).

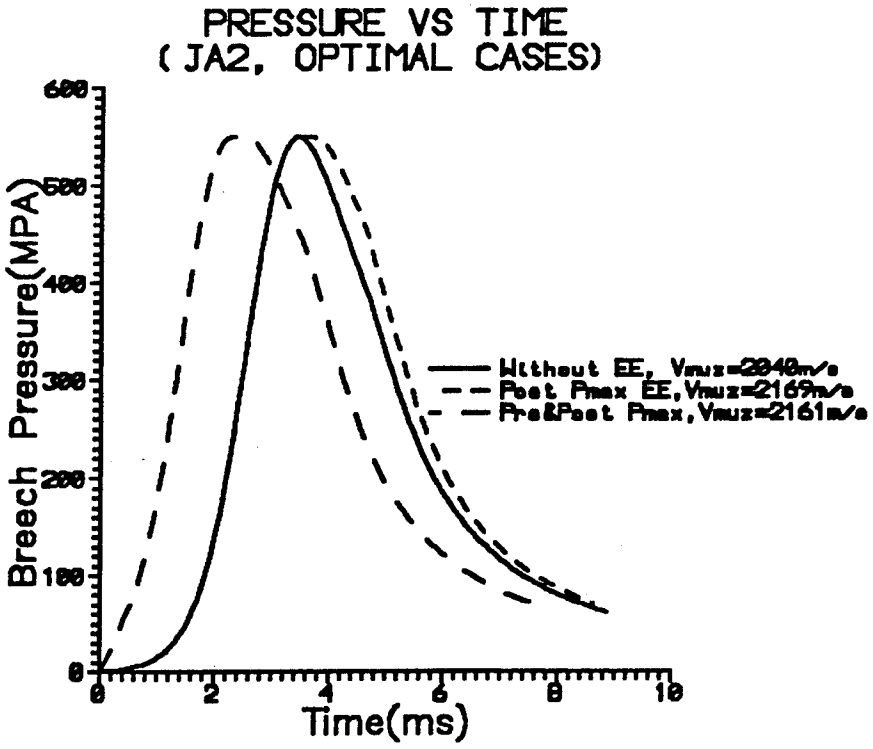

Figure 8. Pressure vs. time (JA2, pre- and post-Pmax).

A summary of the best performances for the conventional SP gun, post-Pmax plasma injection and pre- and post-Pmax plasma injection of the SPETC gun, are listed in Table 13.

Table 13. Optimal Performances

	Conventional	Post-Pmax SPETC	Pre- and Post-Pmax SPETC
EE and Power	0 MJ, 0 GW	5 MJ, 3 GW	5 MJ, 3 GW
M30 Propellant			
Prop. Mass	7.1 kg	7.4 kg	7.3 kg
Web Size	0.1331 cm	0.1433 cm	0.1436 cm
Muzzle Velocity	1,997 m/s	2,139 m/s	2,132 m/s
JA2 Propellant			
Prop. Mass	6.9 kg	7.2 kg	6.9–7.1 kg
Web Size	0.0799 cm	0.0864 cm	0.0824–0.0869 cm
Muzzle Velocity	2,040 m/s	2,169 m/s	2,161 m/s

2.3 PFN Design. Since the plasma resistance history is unknown, all of the circuit designs below are based on the assumption that the plasma resistance is equal to an average value of 25 mΩ.

2.3.1 PFN for Post-Pmax Plasma Injection. There are several combinations of RLC (resistor, inductor and capacitor) circuits which produce the described pulse power shape. The following design is only one suggestion of the pulse power network which will give the approximate desired square pulse power shape used for post-Pmax injection.

This circuit includes six modules. Each module has an equivalent 6,500 μF capacitor, a clamped diode and a 3 μH inductor. With state-of-the-art, high-energy capacitors, the equivalent of 6,500 μF capacitance can be obtained by connecting ten 650 μF capacitors in parallel. If the voltage charge for each capacitor is 17 kV, the energy of the system will be 5.6 MJ and the 5 MJ of energy transferred to the plasma is approximately 93%. This number (93%) is obtained by assuming no power losses in transmission lines. The circuit diagram and its pulse power shape are given in Figures 9–10 respectively.

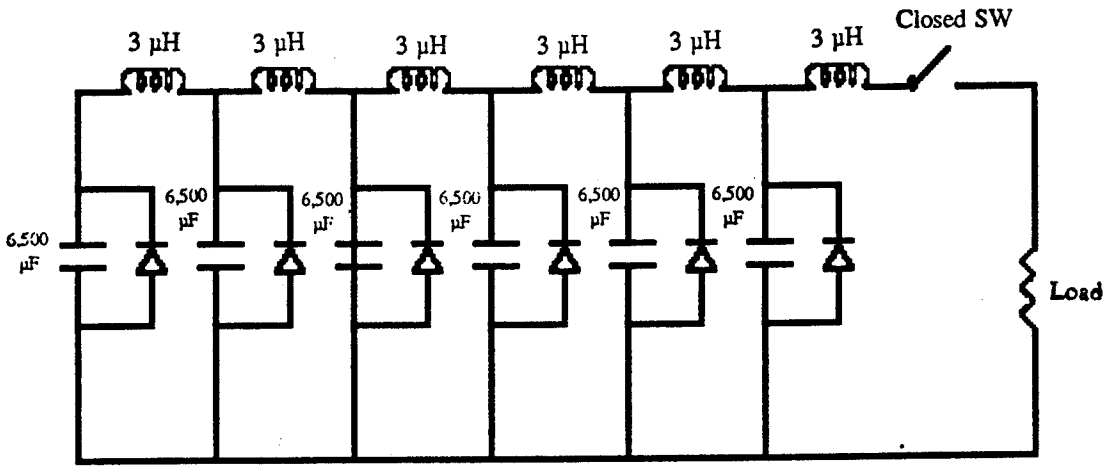

Figure 9. PFN diagram for post-Pmax plasma injection.

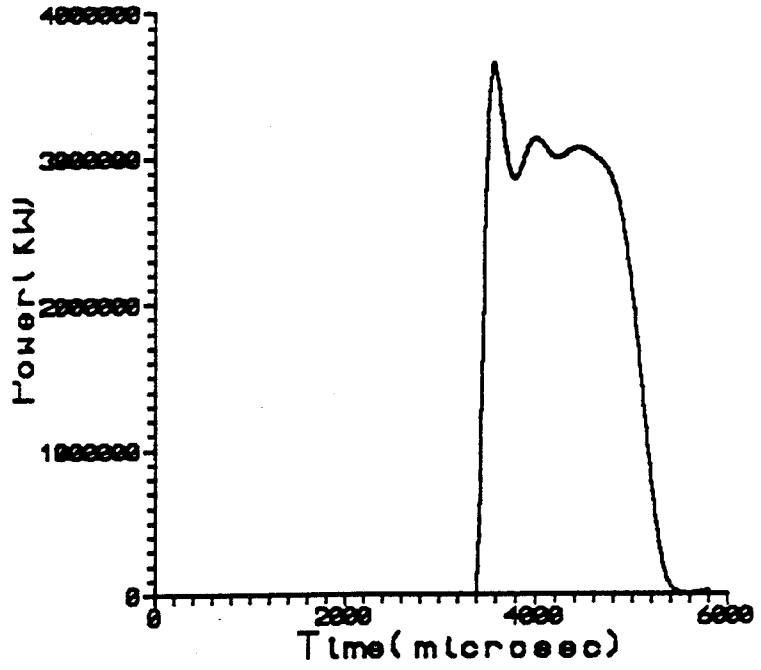

Figure 10. Designed pulse power shape for post-Pmax injection.

2.3.2 PFN for Pre- and Post-Pmax Plasma Injection. As shown in Figure 7, the desired pulse power shape for pre- and post-Pmax injection has two separated pulses: the prepulse with low power for the ignition and a main square power pulse starting at 2.2 ms for a broader pressure profile. The circuit diagram of the PFN which gives approximately this pulse power shape is shown in Figure 11. Basically, this circuit is the same as the circuit for post-Pmax plasma injection except for an additional module which provides the prepower pulse. This additional module is connected to the plasma capillary (load) by two different switches in series: one is open and the other is closed. The open switch serves as a device to disconnect the additional module after its capacitors complete the discharge. The purpose of this disconnection is to prevent recharging of the capacitors from the other modules. The power shape of this PFN, with a constant 25 mΩ load, is shown in Figure 12. If the capacitors are charged up to 16.6 kV, the energy delivered to the load will be 5 MJ after 5.8 ms thus providing 93% efficiency, again assuming the losses on the transmission lines are negligible.

2.3.3 Pros and Cons for Post-Pmax and Pre- and Post-Pmax Plasma Injections. As discussed before, there is no significant difference between the optimal performance or power efficiency of post-Pmax plasma injection and pre- and post-Pmax plasma injection for the SPETC gun. However, there are some advantages and disadvantages between these two methods.

For post-Pmax plasma injection, the PFN is simplier and easier to control. However, this system needs both a conventional igniter and a plasma capillary. A redesigned plasma nozzle is also needed so that propellant gases in the combustion chamber do not flow into the capillary as the result of a pressure gradient between the breech and inside the capillary. Propellant gases inside the plasma capillary could cause difficulty in starting the plasma generation at the later time.

On the other hand, pre- and post-Pmax plasma injection has a more complicated PFN. The separated time of more than 1 ms between the first and second pulse could cause difficulty in starting the plasma jet a second time. The severity of this problem can be determined by experiment. This gun system might also need a redesigned plasma capillary nozzle for the same reason as for post-Pmax plasma injection.

In general, neither of these methods is superior to the other. Considering weight and volume, an additional conventional igniter might be better than an additional RLC circuit module. However, adding a conventional igniter to the gun system can be more complicated than adding one more circuit module to the PFN. Hence, a pre- and post-Pmax plasma injection in which the duration of the first pulse is long enough so that the second pulse does not have difficulty in reigniting the plasma could be a compromise solution.

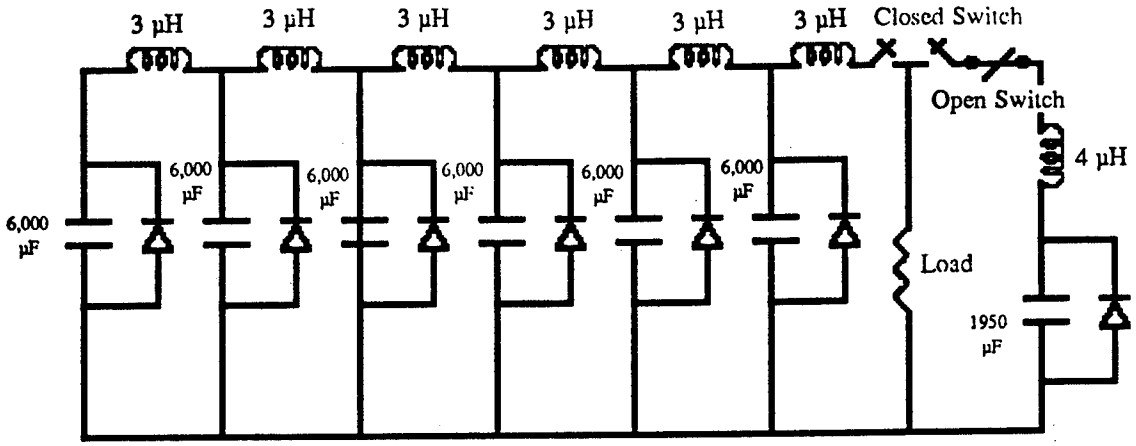

Figure 11. PFN circuit diagram for pre- and post-Pmax plasma injection.

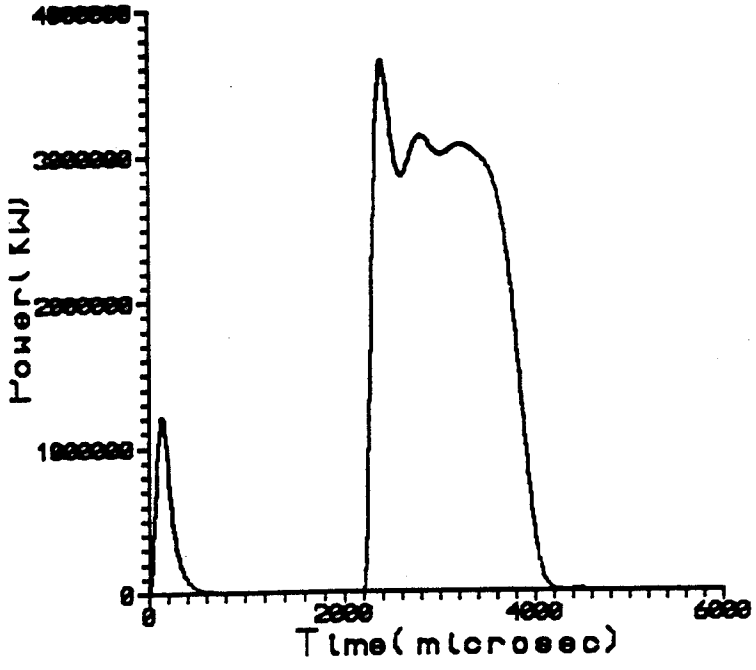

Figure 12. Designed pulse power shape for pre- and post-Pmax plasma injection.

3. ELECTRICAL ENERGY AND POWER TRADE-OFFS

The trade-offs between electrical energy and power supply characteristics are investigated parametrically. Gun performance is calculated as a function of electrical energy, power level, and propellant mass. Two test matrices were examined. The first matrix is performed with the electrical energy ranging from 3.0 MJ to 6.0 MJ, which has a square pulse power shape, the maximum power varying from 2.0 GW to 6.0 GW and the loading density varying from 1.0 g/cm^3 to 1.3 g/cm^3. The second matrix is a more detailed examination from a practical point of view, based on the current power supply capability at the SNRC ETC facility. The electrical energy ranges from 0.2 MJ to 3.0 MJ, maximum power varies from 0.4 GW to 1.6 GW, and propellant mass varies from 6.8 kg to 8.4 kg (loading density is in the range of 0.95 g/cm^3 to 1.2 g/cm^3). The test matrix for electrical energy and power trade-off is listed in Table 14. The gun and propellant characteristics are shown in Table 1; M30 propellant thermochemical values are used in these calculations.

The muzzle velocity vs. power from test 1 for each loading density for 7-perf M30 propellant with different electrical energies are plotted and shown in Figures 13–16. Three-dimensional graphs of muzzle velocity vs. electrical energy and power at loading density 1.0 g/cm^3–1.3 g/cm^3 are also shown in Figures 17–20. Figure 21 is a sample of muzzle velocity vs. power with different loading densities.

As shown in Figures 13–16, the gun performance is directly proportional to the electrical energy input as well as to the electrical power regardless of loading density. The higher the electrical energy supplied, the better the muzzle velocity achieved. Also, for a given energy, the larger input power delivered over a smaller period of time, the higher the velocity obtained. However, it is noted that the efficiency of conversion of electrical energy to muzzle kinetic energy (electrical enhancement factor [EEF]) will drop as electrical energy increases. In addition, the model assumptions imply an instantaneous effect of the plasma from the breech to projectile base. A temperature constraint is not considered in these calculations.

For example, note the intersection of horizontal and vertical lines from Figure 13. With the same loading density - 1.0 g/cm^3, a muzzle velocity of 2,178 m/s can be theoretically achieved by adding 5.0 MJ electrical energy, 4.0 GW power (pulse duration 1.25 ms) or 6.0 MJ electrical energy, 2.7 GW power (pulse duration 2.22 ms) into the combustion chamber. This implies that the later case needs 20%

Table 14. Test Matrix for Energy and Power Trade-Offs Investigation

	Test 1	Test 2
Electrical energy	3.0 MJ–6.0 MJ	0.2 MJ - 3.0 MJ
Power	2.0 GW–6.0 GW	0.4 GW–1.6 GW
Propellant mass	7.1 kg–9.3 kg	6.8 kg–8.4 kg
Loading density	1.0 g/cm^3–1.3 g/cm^3	0.95 g/cm^3–1.2 g/cm^3

more electrical energy to obtain the same muzzle velocity as the previous case. However, one practical disadvantage is that magnetic forces due to the larger current of the earlier system (4 GW) will exceed those of the later system (2.7 GW) by 33%. That might require more spaces or more insulations between components. Furthermore, the electrical energy and power trade-offs can be looked at another way. With the same electrical energy (6 MJ), a short pulse duration of 1 ms can give a muzzle velocity of around 2,208 m/s. This muzzle velocity is improved 1.5% compared to the muzzle velocity with the pulse duration of 2.22 ms. However, muzzle velocity appears to approach an asymptote as a result of the trade-offs between electrical energy and power as observed by the flattening of the power-vs.-velocity curves in Figures 13–16.

Using results from test matrix 2, muzzle velocity vs. propellant mass for electrical energies of 1.0 MJ, 2.0 MJ, and 3.0 MJ with different maximum power are plotted in Figures 22–24 respectively. These graphs again reinforce the results from test 1 about the trade-offs between electrical energy and power supply. The optimal loading density is around 1.0 g/cm^3, and gun performance is decreased rapidly with the increase of loading density beyond the optimal point.

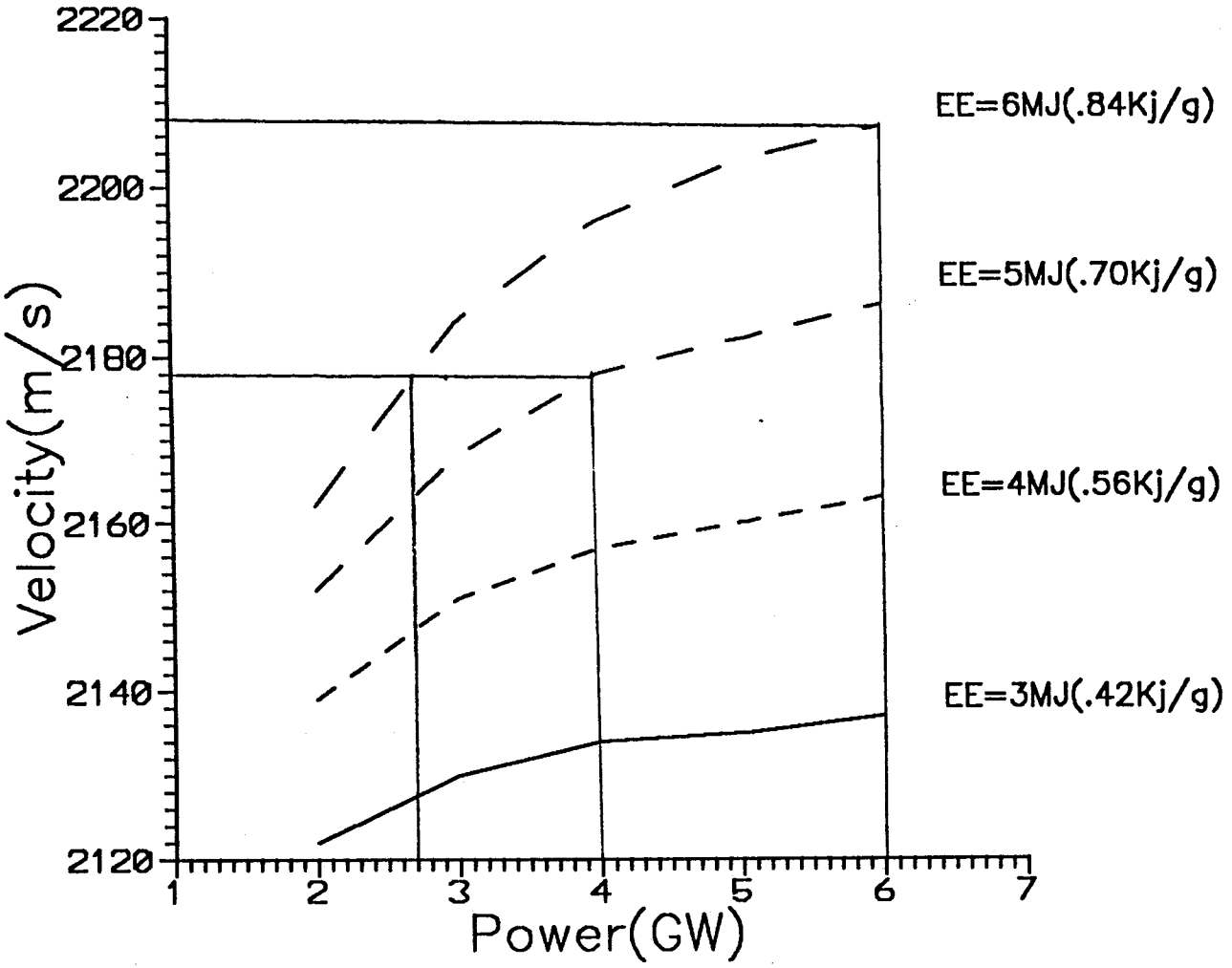

Figure 13. Muzzle velocity vs. power (loading density = 1.0 g/cm^3).

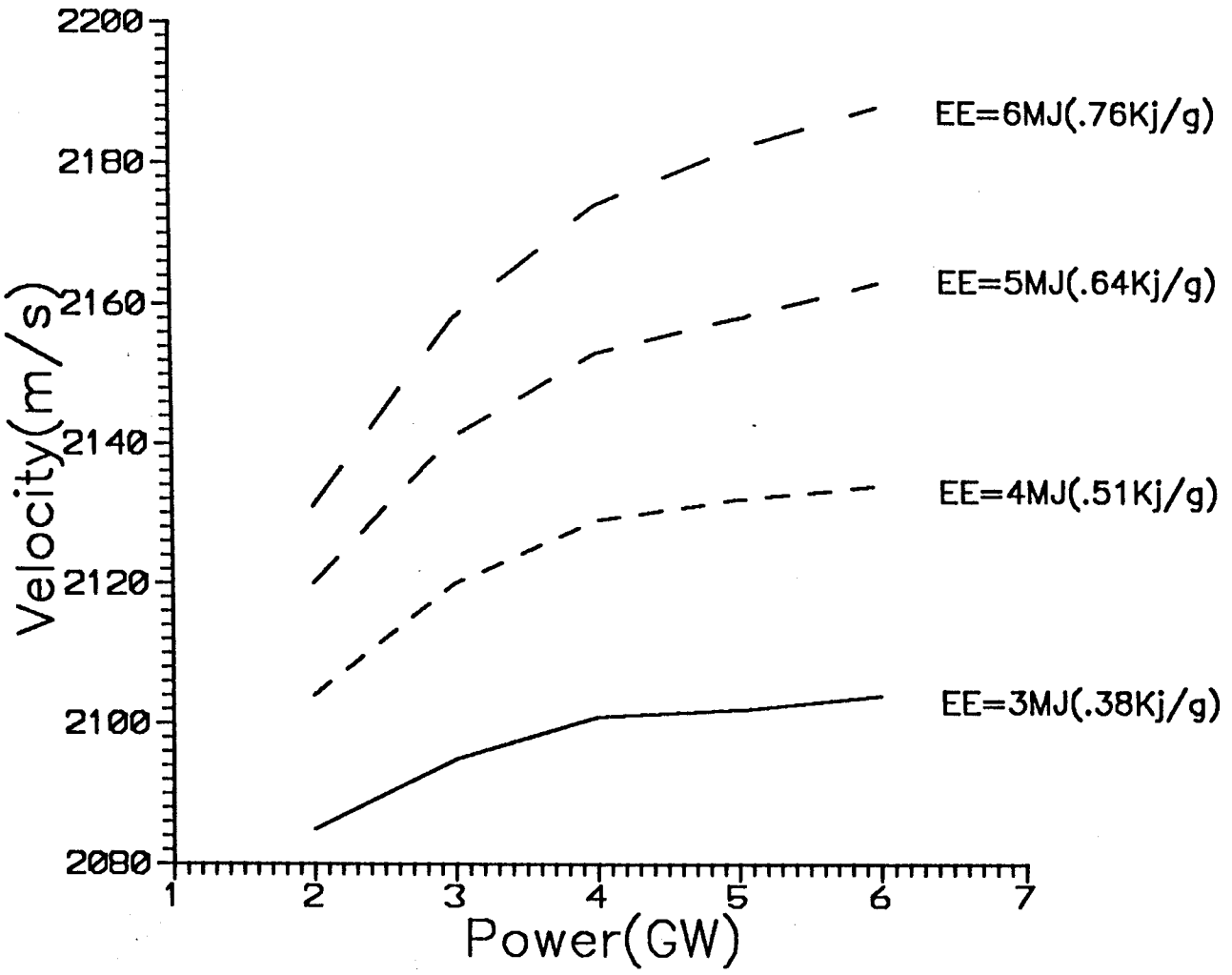

Figure 14. Muzzle velocity vs. power (loading density = 1.1 g/cm^3).

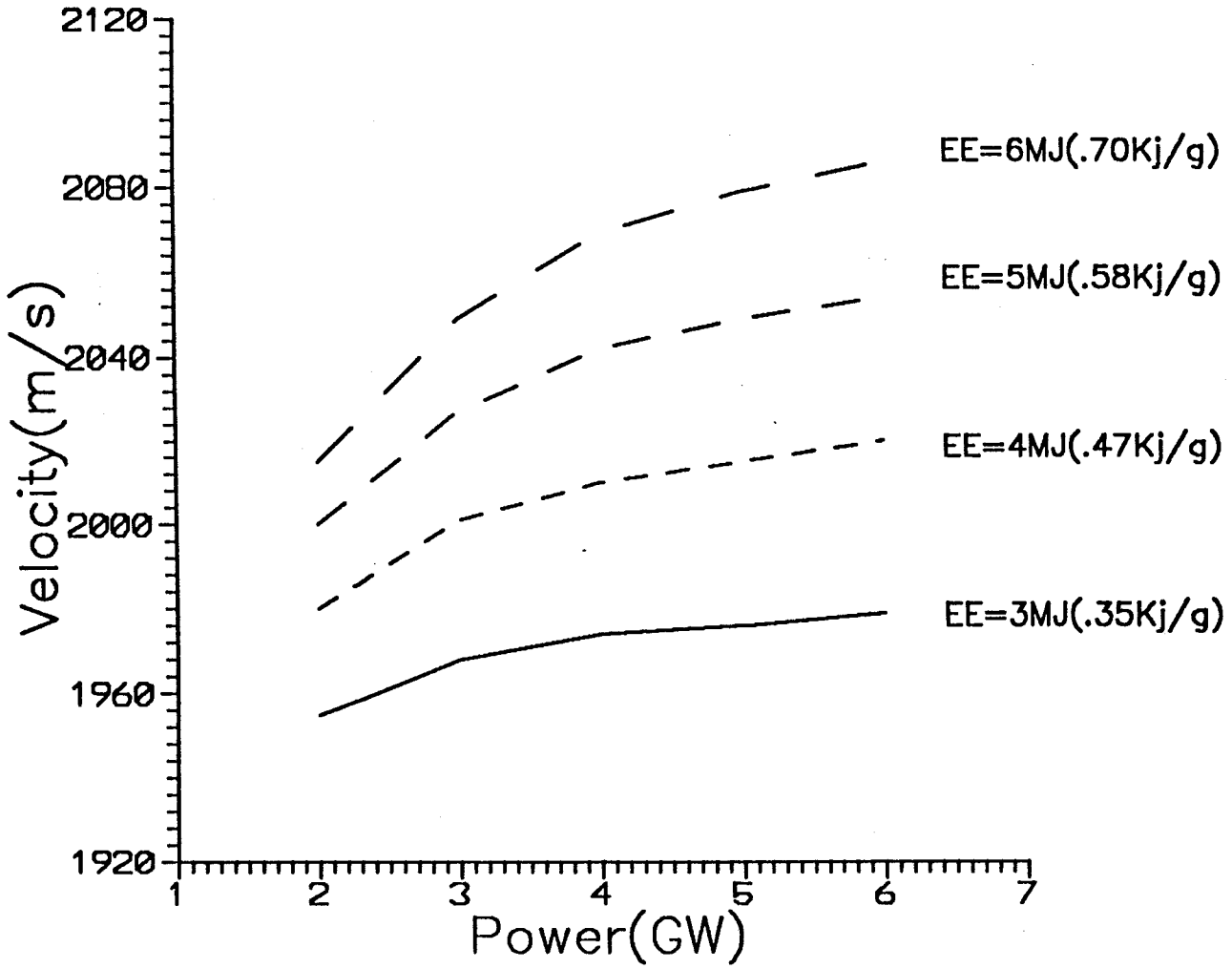

Figure 15. Muzzle velocity vs. power (loading density = 1.2 g/cm^3).

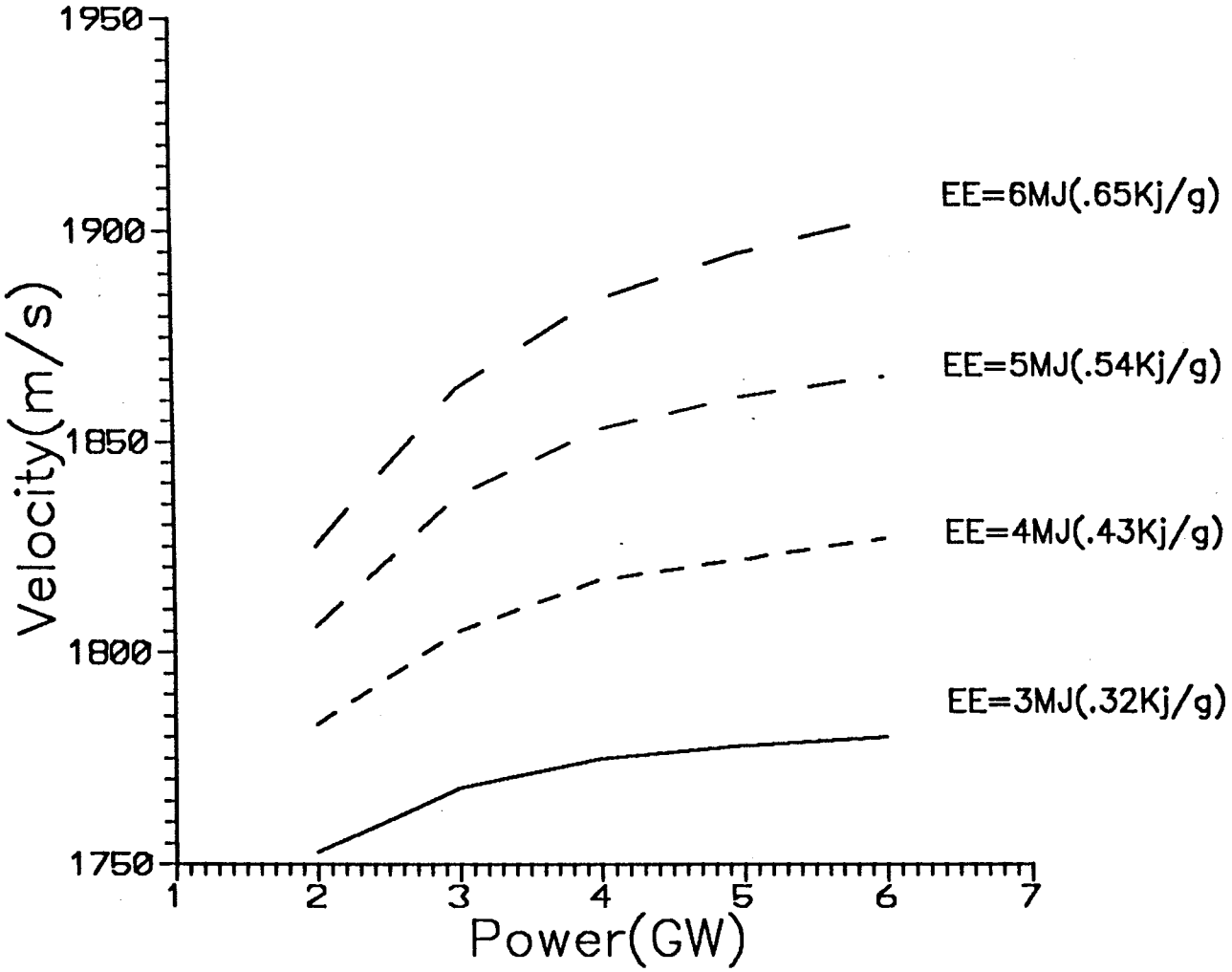

Figure 16. Muzzle velocity vs. power (loading density = 1.3 g/cm^3).

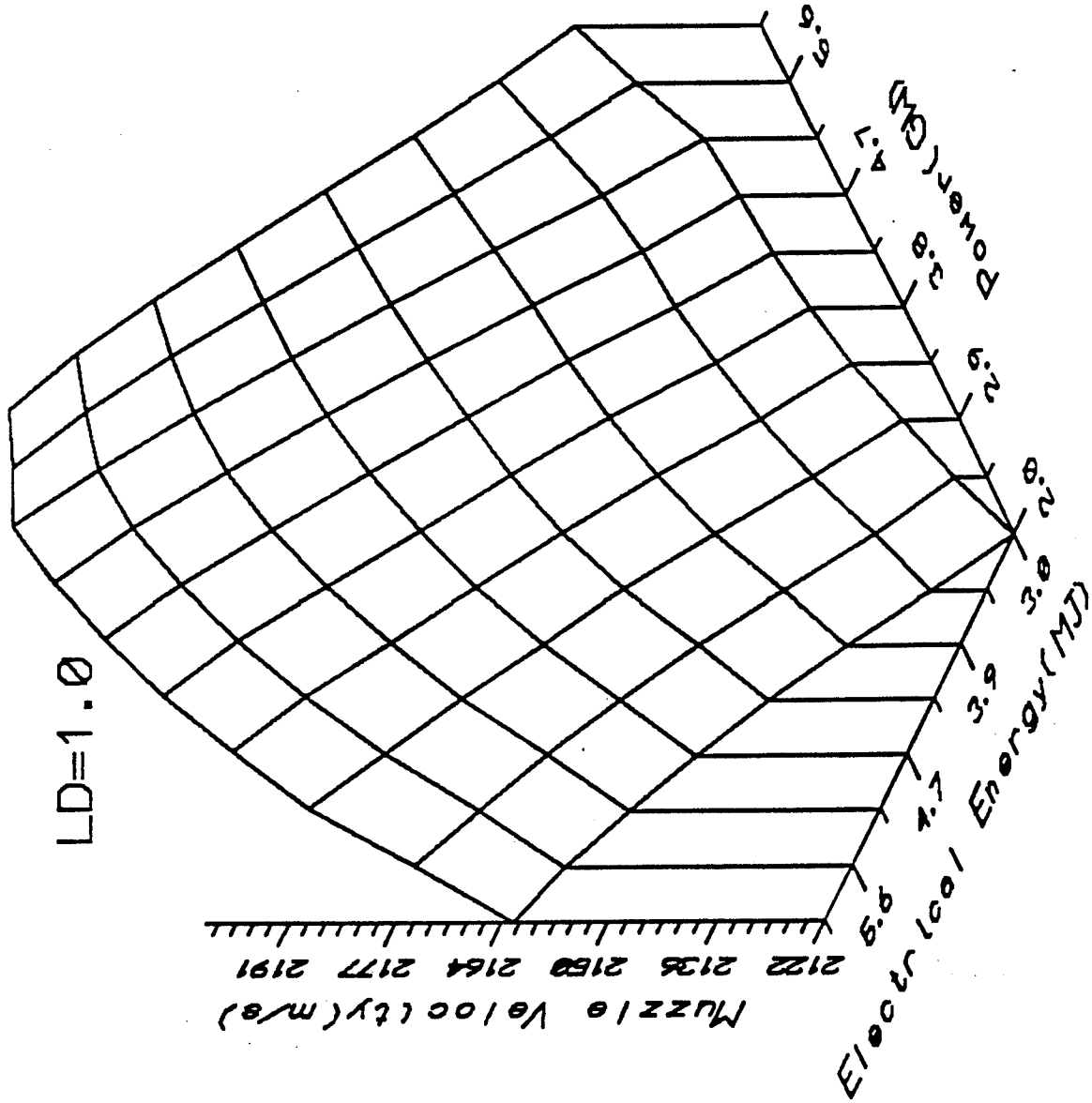

Figure 17. Muzzle velocity vs. electrical energy and power (loading density = 1.0 g/cm^3).

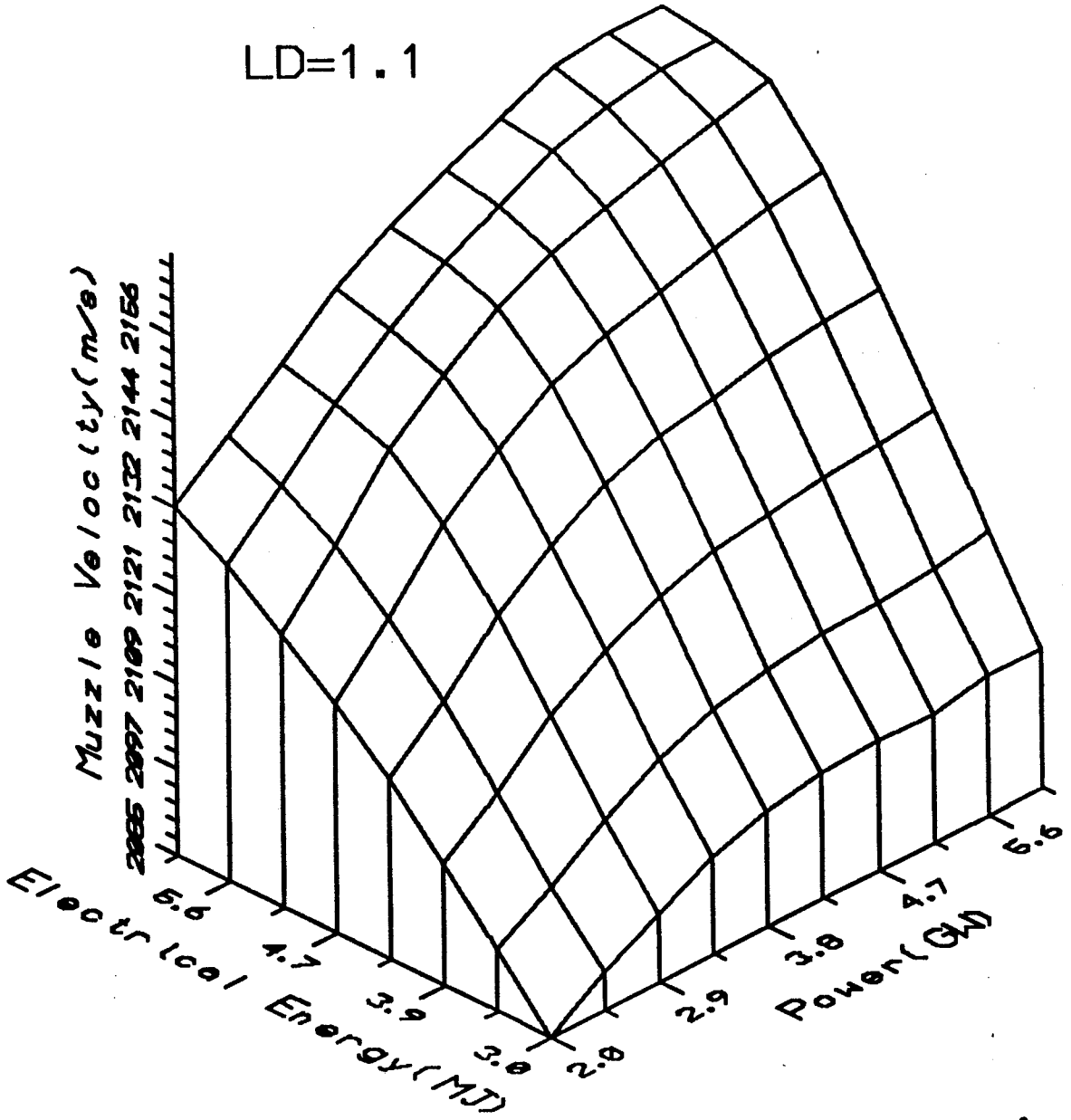

Figure 18. Muzzle velocity vs. electrical energy and power (loading density = 1.1 g/cm^3).

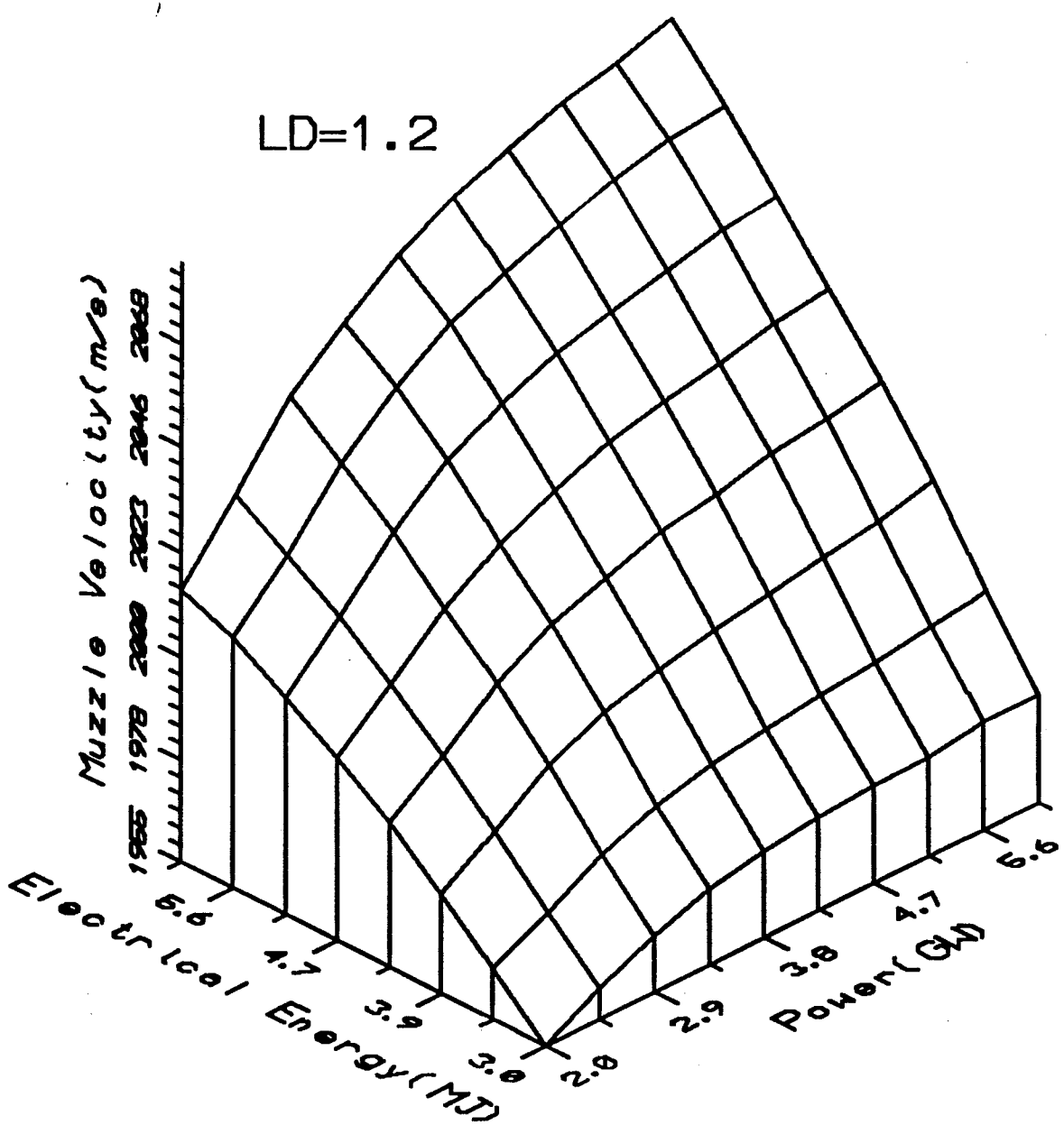

Figure 19. Muzzle velocity vs. electrical energy and power (loading density = 1.2 g/cm^3).

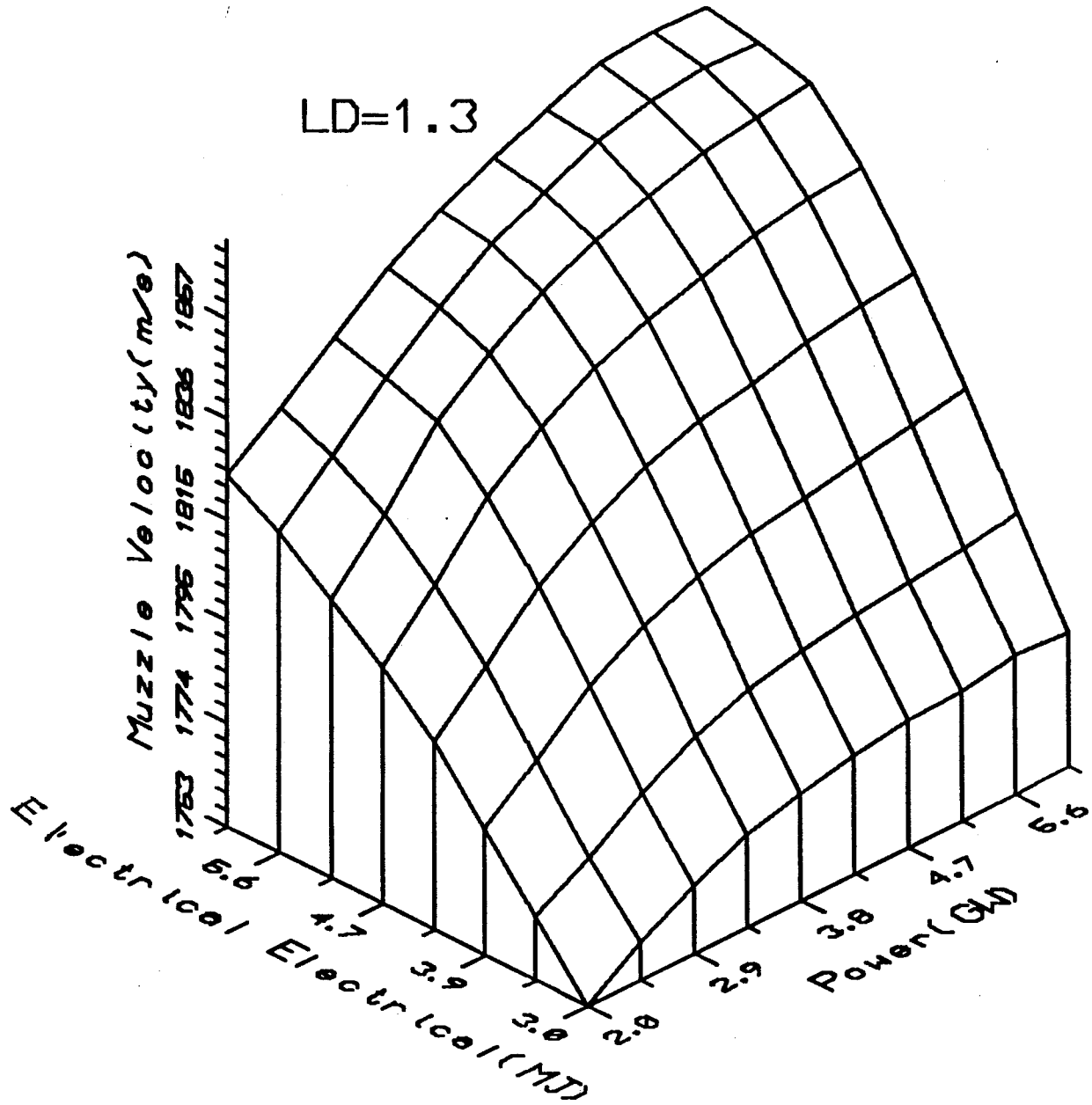

Figure 20. Muzzle velocity vs. electrical energy and power (loading density = 1.3 g/cm^3).

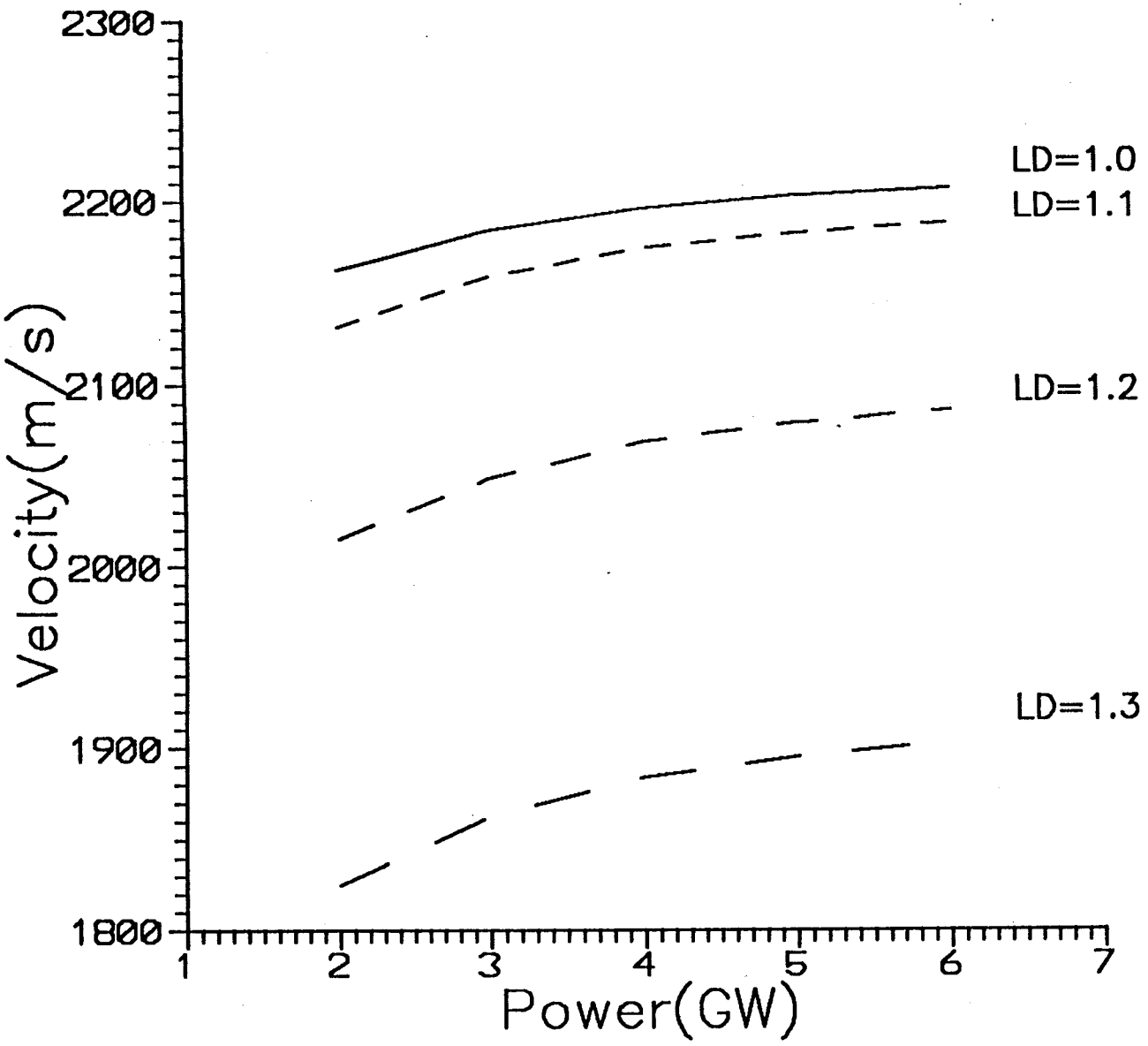

Figure 21. Muzzle velocity vs. power with various loading densities.

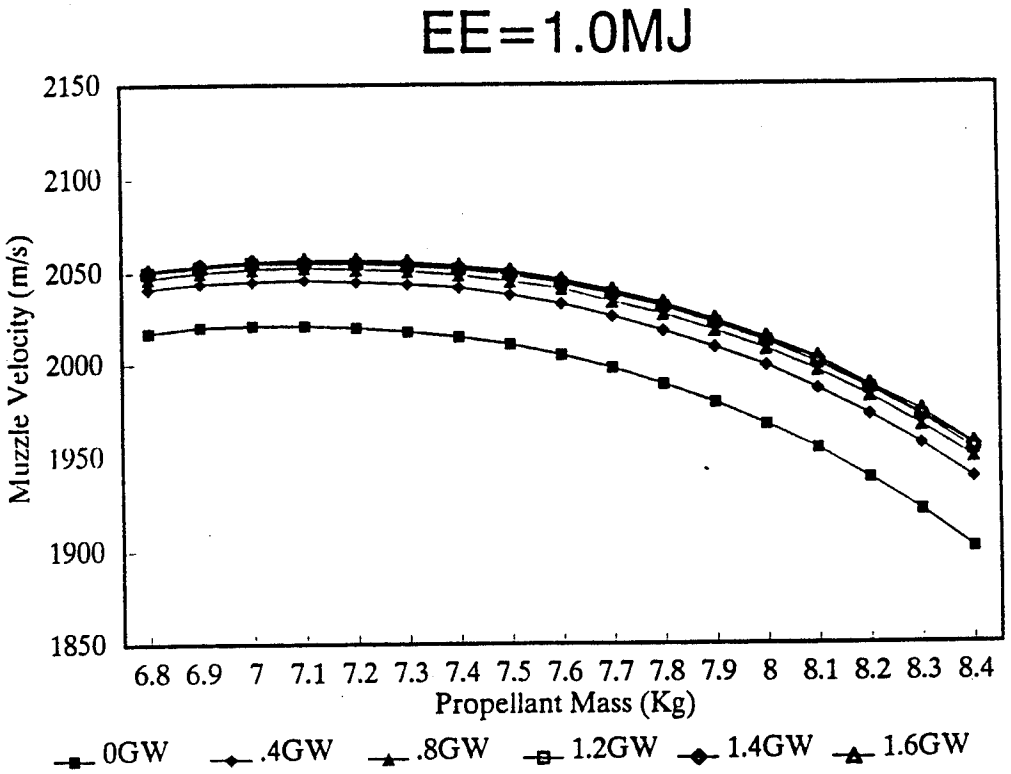

Figure 22. Muzzle velocity vs. propellant mass with various power and EE = 1.0 MJ.

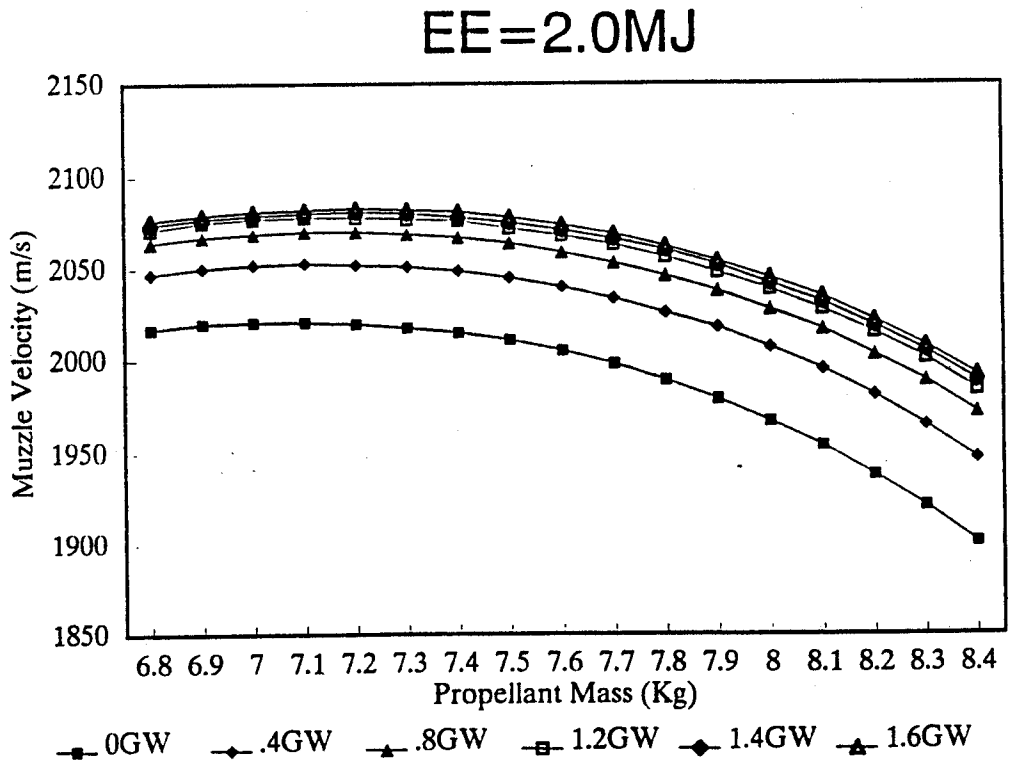

Figure 23. Muzzle velocity vs. propellant mass with various power and EE = 2.0 MJ.

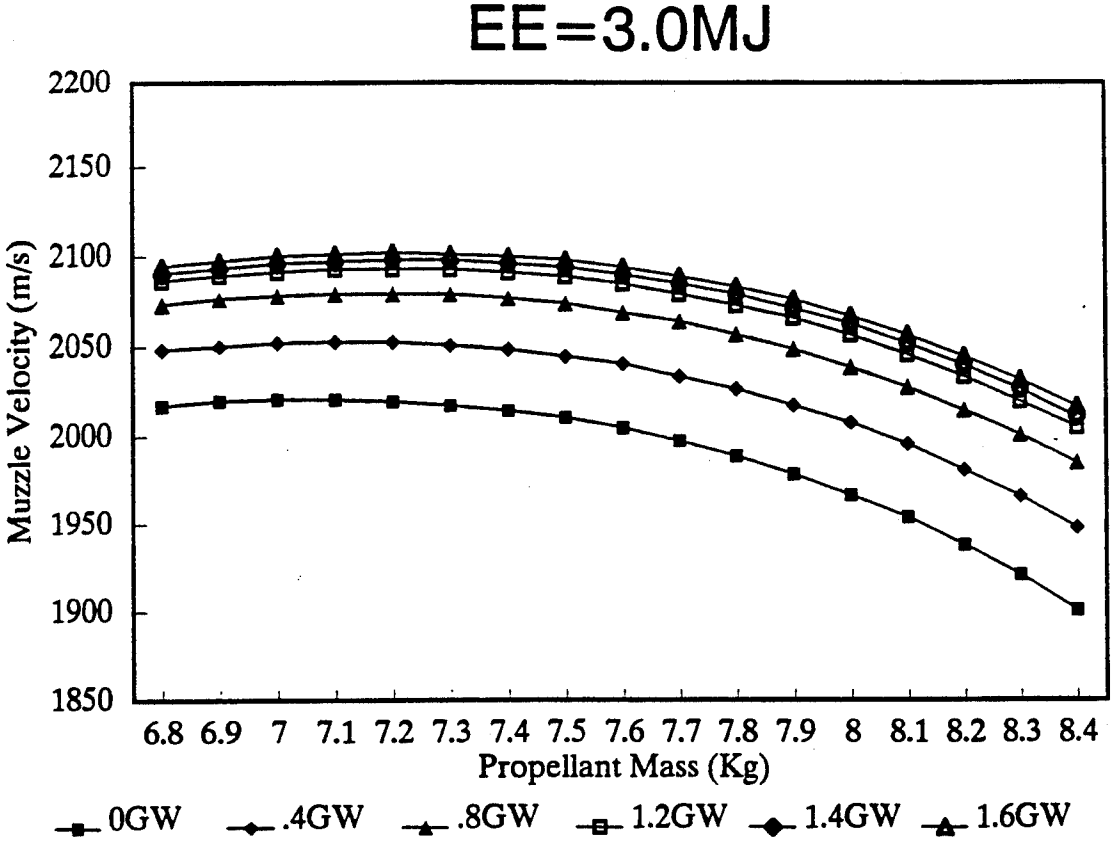

Figure 24. Muzzle velocity vs. propellant mass with various power and EE = 3.0 MJ.

4. PROGRESSIVITY

The progressivity of the propellant charge can be altered in various ways: geometrically as in traditional SP charges; chemically as in deterred propellant or electrically. It was hypothesized that the propellant progressivity could be exploited through the addition of electrical energy. Thus, more progressive geometries such as 19-perf grain might be expected to offer different trade-offs in electrical energy and power than less progressive grain such as 7-perf propellant. Several approaches were used to perform this study and are discussed in the following sections.

4.1 SPETCIB Model. A set of simulations using the SPETCIB model was performed with 1-, 7-, 19-, and 37-perf JA2 propellant. An arbitrary electrical energy and power input was chosen for this study (i.e., 3 MJ electrical energy and 1.6 GW power). The gun performance is shown in Table 15. From this table we can see that the performance can be improved almost 4% by using 37-perf propellant as opposed to 1-perf propellant. However, there is no performance improvement between 7-perf and 19-perf propellant. This is because in both cases the electrical energy serves to supplement the grain progressivity to obtain nearly equivalent pressure-time curves (see Figure 25).

Table 15. Gun Performance With Varying SP Perforation and Propellant Mass (3 MJ, 1.6 GW)

Prop. Mass (kg)	Muzzle Velocity (m/s)			
	1 perf	7 perf	19 perf	37 hex.
7.0	2,063	2,100	2,100	2,130
7.1	2,062	2,100	2,101	2,133
7.2	2,055	2,100	2,102	2,135
7.3	2,053	2,099	2,101	2,135
7.4	2,046	2,096	2,098	2,136

4.2 IBHVG2 Model.

4.2.1 Test 1: The objective of this study is to determine if grain progressivity and post-Pmax plasma pulse power supply can work together to optimize gun performance at higher loading densities.

This problem is approached by using the optimization capabilities of the IBHVG2 model (Frickie and Anderson 1987). The maximization of gun performance was carried out by parametrically varying propellant mass, web size, pulse power profile, and the time to inject pulse power to combustion chamber after maximum breech pressure.

The gun parameters for this study are the same as listed in Table 1, except maximum pressure (500 MPa), chamber volume (6,704 cm^3), and projectile mass (4.9 kg) are based on the current gun testing at Eglin AFB, and only propellant M30 is investigated.

A 250-MW power pulse for 4 ms (1 MJ) is added at the beginning of the ballistic cycle; web size and charge mass are varied to obtain the optimal performance. The best performance for 1-perf grain is 1,776 m/s at charge weight 5.5 kg and for 37-perf hex. is 1,866 m/s with charge weight 6.6 kg. A second power pulse of 2 MJ is added at different times after Pmax. The optimal muzzle velocity with a short power pulse of 0.5-ms pulse duration for 1 perf is 1,855 m/s with charge weight 5.6 kg, and for 37 perf is 1,935 m/s with the charge weight 6.6 kg. In the sense of optimal loading density, with 2 MJ electrical

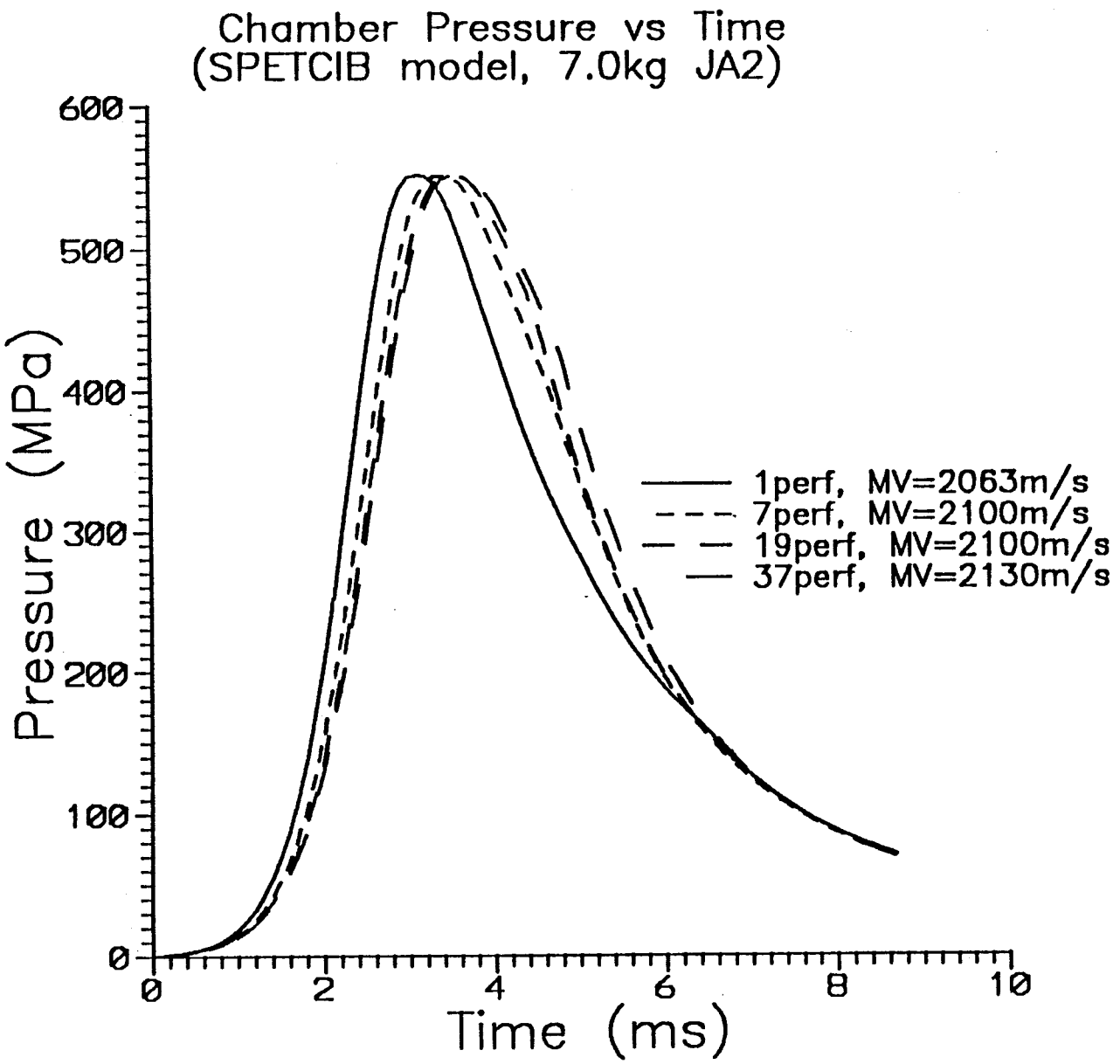

Figure 25. Pressure vs. time with various perforations (SPETCIB model, 7.0 kg JA2).

energy supply, the optimal charge mass for 37-perf hex. grain is 1 kg or 18% heavier than the optimal charge mass of 1-perf grain, and the percent difference between these muzzle velocities is 4.3%. However, with the same grain geometry, 2 MJ does not give a significant difference in the optimal propellant mass. The results again show that, under the conditions studied with conventional propellants, an increase in the electrical energy level results in only a marginal increase in optimal loading density. Thus, modifications to the propellant such as deterrents are necessary in order to exploit higher charge masses.

The pressure profiles for the best performances of 1 perf and 37-perf hex. propellants are shown in Figures 26–27 respectively.

4.2.2 Test 2. The objective of this test is to see what needs to be done to the plasma power and energy in order to usefully burn 15% and 25% more charge mass over the optimal SP loading density. This problem is approached by increasing the charge mass by 15% and 25% over the optimal charge mass baseline and then adding an arbitrary level of power and energy in order to find the right combination of power and energy to consume all the extra charge mass.

For 1-perf grain, 15% over optimal baseline 5.5 kg is 6.3 kg, and 25% is 6.825 kg of propellant. For 37-perf hex. grain, these 15% and 25% over 6.6 kg will be 7.59 kg and 8.25 kg propellant respectively. The results of this test are listed in Table 16.

As we can see in Table 16, although the rate and the amount of electrical energy affect muzzle velocity, it is difficult to burn 25% more charge mass than the SP optimal case even under ideal conditions.

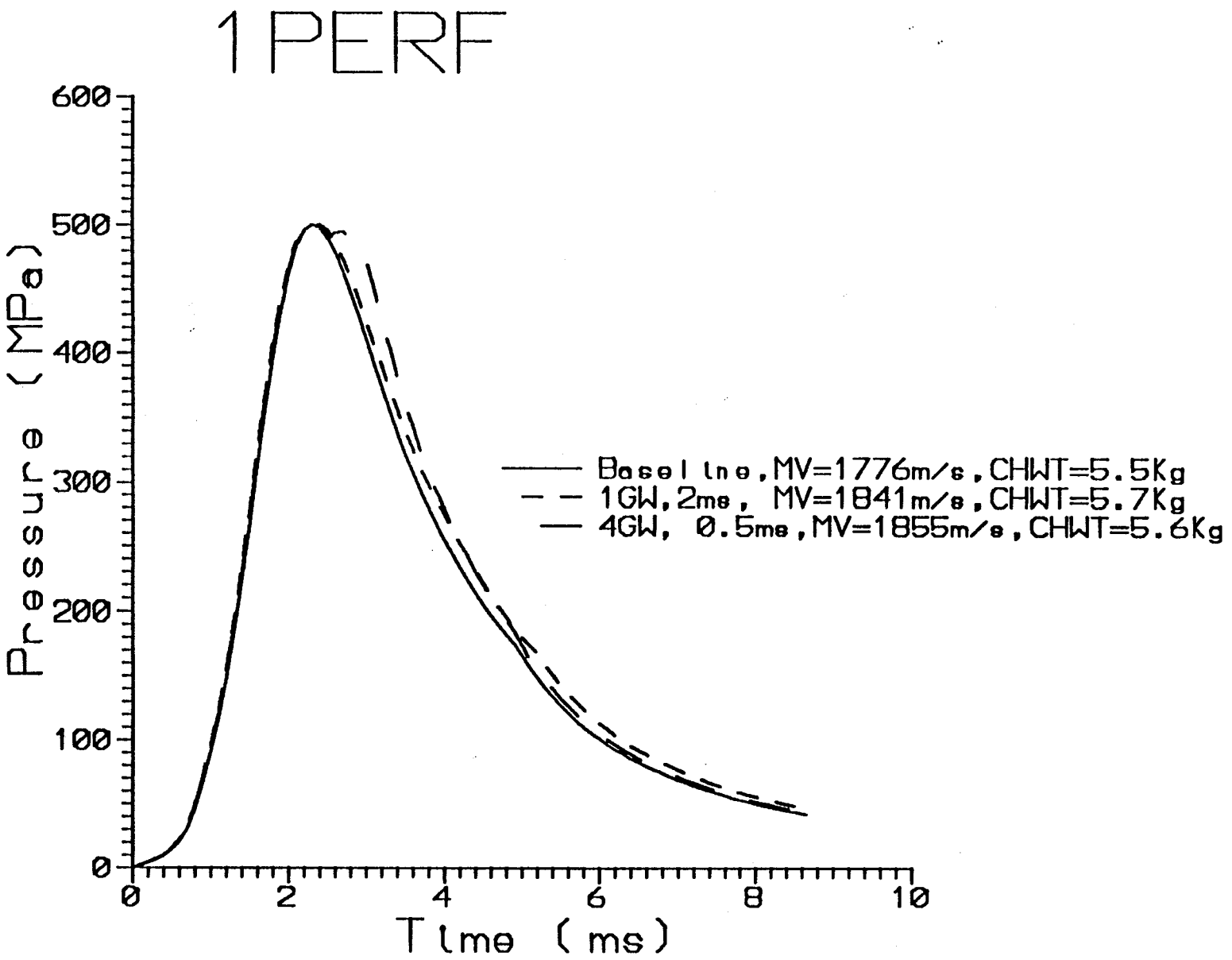

Figure 26. Pressure vs. time (M30, 1 perf).

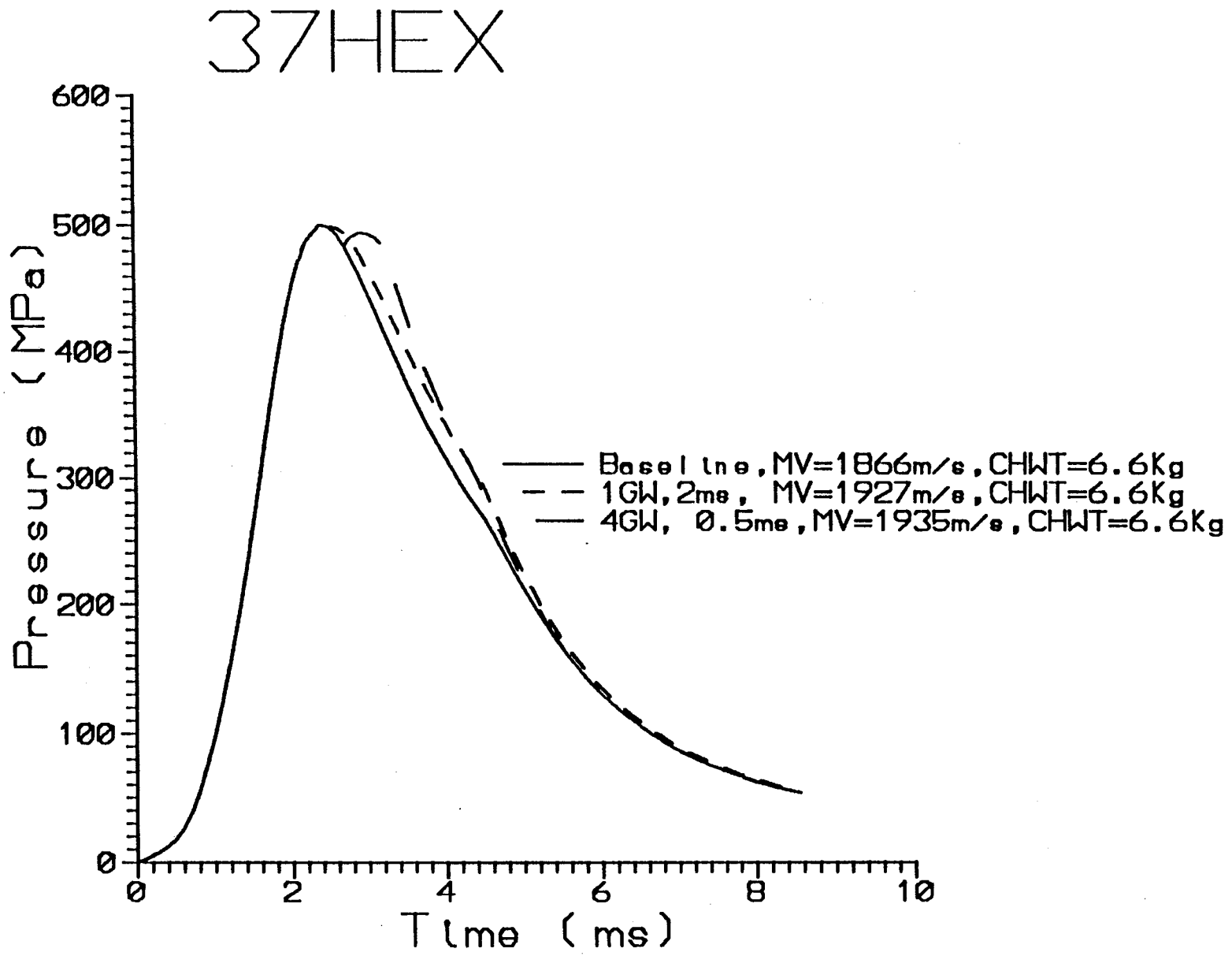

Figure 27. Pressure vs. time (M30, 37 perf).

Table 16. Summary of Study on the Effect of Electrical Energy Level on Propellant Burnt With 500 MPa Pmax

Prop. Mass (kg)	Elect. Energy Added 1-ms Duration (MJ)	Muzzle Velocity (m/s)	Prop. Burnt Fraction
1 perf			
5.5 (baseline)	0	1,776	1.00
6.3 (15% more)	0	1,737	1.00
6.3	2	1,815	1.00
6.3	4	1,896	1.00
6.3	6	1,941	1.00
6.3	8	2,002	1.00
6.9 (25% more)	0	1,649	0.88
6.9	2	1,712	0.90
6.9	4	1,815	0.92
6.9	6	1,890	0.93
6.9	8	1,921	0.95
6.9	10	1,981	0.96
6.9	12	2,039	0.97
6.9	14	2,095	0.98
6.9	16	2,135	0.99
6.9	18	Model cannot adjust the web to meet Pmax.	—
37 perf			
6.6 (baseline)	0	1,866	1.000
7.59 (15% more)	0	1,800	0.996
7.59	2	1,886	0.998
7.59	4	1,949	0.999
7.49	6	2,016	1.000
8.25 (25% more)	0	1,662	0.895
8.25	2	1,762	0.923
8.25	4	1,853	0.941
8.25	6	1,895	0.957
8.25	8	1,962	0.966
8.25	12	1,978	0.976
8.25	16	2,066	0.985
8.25	20	2,149	0.991
8.25	22	2,189	0.993
8.25	24	2,196	0.994

4.3 Comparison Between the Gun Performance From the IBHVG2 Calculation and From the CONPRESS Calculation. Although the simulations performed previously with the IBHVG2 do not indicate substantial performance increase through a combination of progressivity, loading density, and electrical energy, the study is somewhat limited by the assumption of "traditional" ballistics. Therefore, in order to determine maximum performance possible under the constraint of Pmax, a constant pressure calculation for M30 propellant and 3-MJ electrical energy is shown in Figure 28. The simulation is performed with CONPRESS (Oberle 1993) and removes the progressivity constraint inherent in the IBHVG2 calculations. As can be seen in Figure 28, a significant increase in muzzle velocity appears possible for loading densities approaching the material density of the propellant. This is due to the fact that more energy is supplied to the system. The difference between the IBHVG2 and the CONPRESS predicted muzzle velocities for a given loading density surmountable through proper tailoring of the gas generation rate of the propellant. Figure 28 implies that radically new progressivities are needed to approach ideal performance. The electrical energy can potentially be used to control the process.

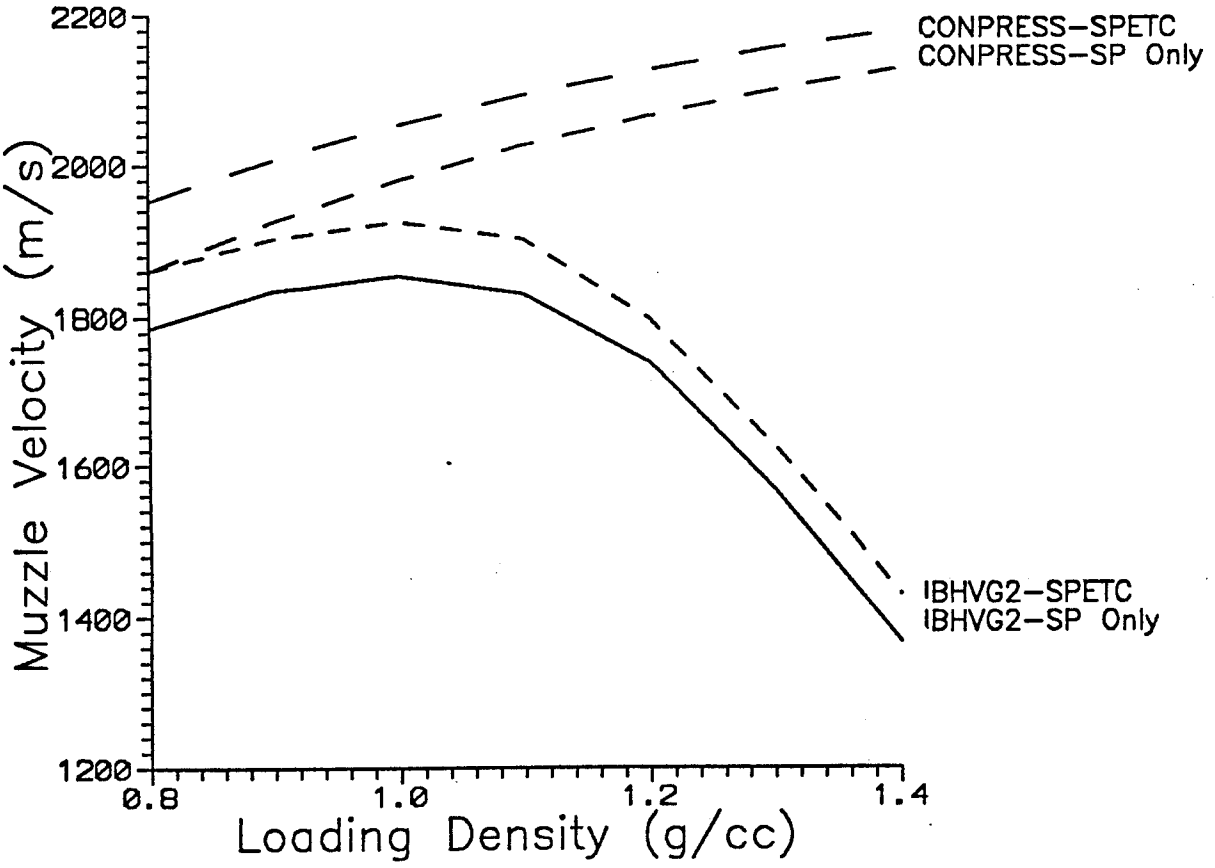

Figure 28. Muzzle velocity vs. loading density from the IBHVG2 and the CONPRESS calculations (M30 propellant, 37 perf, EE = 3 MJ).

5. CONCLUSIONS

In the 105-mm gun envelope studied with M30 and JA2 propellants,

(1) The optimal web for the conventional SP gun can be seen as also the optimal web for the post-Pmax plasma injection SPETC gun using a given standard propellant. The difference between these two optimal web sizes is negligible as shown in section 1.

(2) There is a trade-off between electrical energy and power supply for equivalent performance. With the same total electrical energy supply, shorter pulse power duration gives better muzzle velocity. From a practical point of view, it can be seen in two different aspects: (a) The electrical power supply system can be significantly downsized by choosing an appropriate pulse power duration for the same muzzle velocity assuming the larger power levels do not create practical problems such as mechanical stress, etc., and (b) The flexibility of pulse power duration is quite important in designing a PFN, especially for experiments in the laboratory.

(3) A near-optimal muzzle velocity for this gun envelope under the constraint of maximum pressure is predicted with a 7-perf grain and 3 MJ of electrical energy using standard propellants. Although some performance enhancement is possible through the variation of grain geometry (i.e., number of perfs), loading density, electrical energy, and power, the increase is small for conventional propellants. This result may appear counterintuitive; however, the Pmax constraint fixes the specific web and, for standard SPs, also determines the progressivity after Pmax. Although there is a progressivity increase as the number of perfs increase, the charge is not sufficient to substantially alter the rapid pressure decay after Pmax occurring for the 7-perf grain.

(4) The constant pressure simulations (Figure 28) indicate that significant performance enhancement is possible in this gun envelope under the Pmax constraint with the energy of standard M30 propellant and 3-MJ electrical energy. To achieve the muzzle velocity predicted, the gas generation rate of the propellant must be significantly altered after Pmax. The modification of the gas generation rate is possible through chemical progressivity (such as high-deterred grain), electrical energy augmentation, and novel grain geometries using the electrical energy to control the process. The exploitation of these fields is necessary in order to realize the potential of ETC guns.

INTENTIONALLY LEFT BLANK.

6. REFERENCES

Fickie, K., and R. Anderson. "IBHVG2-A User's Guide." BRL-TR-2829, U.S. Army Ballistic Research Laboratory, Aberdeen Proving Ground, MD, July 1987.

Juhasz, A., K. Jamison, K. White, and G. Wren. "Introduction to Electrothermal Gun Propulsion." Technology Efforts in ET Gun Propulsion, vol.1, FY 88, U.S Army Ballistic Research Laboratory, Aberdeen Proving Ground, MD, December 1988.

Juhasz, A., K. White, H. McElroy, J. R. Greig, and Z. Kaplan. "A Status Report on Solid Propellant ETC." 29th JANNAF Combustion Subcommittee Meeting, NASA Langley Research Center, Hampton, VA, October 1992a.

Juhasz, A., S. Smith, Z. Kaplan, D. Melnik, D. Saphir, and M. Blum. "Solid Propellant Electrothermal Gun Propulsion." U.S. Army Science Conference, Orlando, FL, June 1992b.

Morrison, W. F., G. Wren, and W. Oberle. "Interior Ballistic Modeling of Hybrid Solid Propellant Electrothermal-Chemical Gun." Proceedings of the 28th JANNAF Combustion Meeting, October 1991.

Morrison, W. F., G. Wren, and W. Oberle. "Interior Ballistic Processes in Electrothermal-Chemical Gun." Proceedings of the 13th International Symposium on Ballistics, June 1992.

Oberle, W. F. "Constant Pressure Interior Ballistics Code CONPRESS: Theory and User's Manual." ARL-TR-199, U.S. Army Research Laboratory, Aberdeen Proving Ground, MD, September 1993.

Princeton Combustion Research Laboratories, Inc. "User's Manual: P2SIM." PCRL-TR-92-001, 27 April 1992.

White, K. J., W. F. Oberle, and A. A. Juhasz. "Performance Potential and Limits of Existing Large Caliber Systems When Applying the Electrothermal-Chemical Propulsion Concept." Presented at the 30th JANNAF Combustion Meeting, November 1993.

INTENTIONALLY LEFT BLANK.

NO. OF COPIES	ORGANIZATION
2	ADMINISTRATOR ATTN DTIC DDA DEFENSE TECHNICAL INFO CTR CAMERON STATION ALEXANDRIA VA 22304-6145
1	COMMANDER ATTN AMCAM US ARMY MATERIEL COMMAND 5001 EISENHOWER AVE ALEXANDRIA VA 22333-0001
1	DIRECTOR ATTN AMSRL OP SD TA US ARMY RESEARCH LAB 2800 POWDER MILL RD ADELPHI MD 20783-1145
3	DIRECTOR ATTN AMSRL OP SD TL US ARMY RESEARCH LAB 2800 POWDER MILL RD ADELPHI MD 20783-1145
1	DIRECTOR ATTN AMSRL OP SD TP US ARMY RESEARCH LAB 2800 POWDER MILL RD ADELPHI MD 20783-1145
2	COMMANDER ATTN SMCAR TDC US ARMY ARDEC PCTNY ARSNL NJ 07806-5000
1	DIRECTOR ATTN SMCAR CCB TL BENET LABORATORIES ARSENAL STREET WATERVLIET NY 12189-4050
1	DIR USA ADVANCED SYSTEMS ATTN AMSAT R NR MS 219 1 R&A OFC AMES RESEARCH CENTER MOFFETT FLD CA 94035-1000

NO. OF COPIES	ORGANIZATION
1	COMMANDER ATTN AMSMI RD CS R DOC US ARMY MISSILE COMMAND REDSTONE ARSNL AL 35898-5010
1	COMMANDER ATTN AMSTA JSK ARMOR ENG BR US ARMY TANK AUTOMOTIVE CMD WARREN MI 48397-5000
1	DIRECTOR ATTN ATRC WSR USA TRADOC ANALYSIS CMD WSMR NM 88002-5502
1	COMMANDANT ATTN ATSH CD SECURITY MGR US ARMY INFANTRY SCHOOL FT BENNING GA 31905-5660
	ABERDEEN PROVING GROUND
2	DIR USAMSAA ATTN AMXSY D AMXSY MP H COHEN
1	CDR USATECOM ATTN AMSTE TC
1	DIR USAERDEC ATTN SCBRD RT
1	CDR USACBDCOM ATTN AMSCB CII
1	DIR USARL ATTN AMSRL SL I
5	DIR USARL ATTN AMSRL OP AP L

NO. OF COPIES	ORGANIZATION
1	OSD SDIO IST ATTN DR LEN CAVENY PENTAGON WASH DC 20301-7100
1	CHAIRMAN DOD EXPLOSIVES SAFETY BD HOFFMAN BLDG 1 RM 856 C 2461 EISENHOWER AVE ALEXANDRIA VA 22331-0600
1	DA OFC OF THE PM 155MM HWTZR M109A6 PALADN ATTN SFAE AR HIP IP MR R DE KLEINE PCTNY ARSNL NJ 07806-5000
1	CDR USACECOM R&D TECHNICAL LIBRARY ATTN ASQNC ELC IS L R MYER CENTER FT MONMOUTH NJ 07703-5301
1	PM PEO ARMAMENTS TMAS ATTN AMCPM TMA K RUSSELL PCTNY ARSNL NJ 07806-5000
1	PM PEO ARMAMENTS TMAS ATTN AMCPM TMA 105 PCTNY ARSNL NJ 07806-5000
1	PM PEO ARMAMENTS TMAS ATTN AMCPM TMA 120 PCTNY ARSNL NJ 07806-5000
1	CDR PRODUCTION BASE MODERNIZATION AGENCY ATTN AMSMC PBM E L LAIBSON PCTNY ARSNL NJ 07806-5000
2	DIR BENET LABS ATTN SARWV RD P VOTIS P ALTO WATERVLIET NY 12189
1	CDR US ARMY AMCCOM ATTN AMSMC IRC G COWAN ROCK ISLAND IL 61299-7300

NO. OF COPIES	ORGANIZATION
2	CDR US ARMY AMCCOM ATTN SMCAR ESM R W FORTUNE R ZASTROW ROCK ISLAND IL 61299-7300
1	CMDT USAAS ATTN AVIATION AGENCY FT RUCKER AL 36360
1	DIR HQ TRAC RPD ATTN ATCD MA MAJ WILLIAMS FT MONROE VA 23651-5143
1	CDR USAMC ATTN AMCICP AD MICHAEL F FISETTE 5001 EISENHOWER AVE ALEXANDRIA VA 22333-0001
1	CDR US ARMY ARDEC ATTN SMCAR CCS PCTNY ARSNL NJ 07806-5000
1	CDR US ARMY ARDEC ATTN SMCAR CCH T L ROSENDORF PCTNY ARSNL NJ 07806-5000
1	CDR US ARMY ARDEC ATTN SMCAR CCH V E FENNELL PCTNY ARSNL NJ 07806-5000
1	CDR US ARMY ARDEC ATTN SMCAR AE J PICARD PCTNY ARSNL NJ 07806-5000
2	CDR US ARMY ARDEC ATTN SMCAR AEE B D DOWNS D CHIU PCTNY ARSNL NJ 07806 5000
1	CDR US ARMY ARDEC ATTN SMCAR AEE J LANNON PCTNY ARSNL NJ 07806 5000
1	CDR US ARMY ARDEC ATTN SMCAR AES S KAPLOWITZ PCTNY ARSNL NJ 07806-5000

NO. OF COPIES	ORGANIZATION
3	CDR US ARMY ARDEC ATTN SMCAR FSE T GORA B KNUTELSKY K CHEUNG PCTNY ARSNL NJ 07806-5000
1	CDR US ARMY ARDEC ATTN SMCAR EG R ZIMANY PCTNY ARSNL NJ 07806-5000
2	CDR USARL ATTN TECH LIB D MANN PO BOX 12211 RSCH TRI PK NC 27709
1	CDR USABRDC ATTN STRBE WC TECH LIB VAULT BLDG 315 FT BELVOIR VA 22060-5606
1	CDR US ARMY TRAC DEFENSE LOGISTICS STUDIES FT LEE VA 23801-6140
1	PRESIDENT US ARMY ARTILLERY BD FT SILL OK 73503
1	CMDT USACGSC ATTN STAFF COLLEGE FT LVNWORTH KS 66027-5200
1	CMDT USASWS ATTN REV & TNG LIT DIV FT BRAGG NC 28307
1	CDR RADFORD ARMY AMMO PLANT ATTN SMCRA QA HI LIB RADFORD VA 24141
1	CMDT USAFAS ATTN STSF TSM CN FT SILL OK 73503-5600
2	CDR NGIC ATTN AMXST MC 3 S LEBEAU C BEITER 220 SEVENTH ST NE CHARLOTTESVILLE VA 22901
1	CMDT USAFACAS ATTN ATSF CO MW B WILLIS FT SILL OK 73503

NO. OF COPIES	ORGANIZATION
1	OFFICE OF NAVAL RESEARCH ATTN CODE 473 R S MILLER 800 N QUINCY ST ARLINGTON VA 22217
2	CDR NSSC ATTN SEA 62R SEA 64 WASH DC 20361-5101
1	CDR NASC ATTN AIR 954 TECH LIB WASH DC 20360
1	NAVAL RSCH LAB TECH LIB WASH DC 20375
2	CDR NSWC ATTN J P CONSAGA C GOTZMER SLVR SPRNG MD 20902-5000
2	CDR NSWC ATTN K KIM CODE R 13 R BERNECKER CODE R 13 SLVR SPRNG MD 20902-5000
3	CDR NSWC ATTN 610 C SMITH 6110J K RICE 6110C S PETERS INDIAN HEAD MD 20640-5035
2	CDR NSWC ATTN CODE G33 T DORAN J COPLEY DAHLGREN VA 22448-5000
3	CDR NSWC CODE G30 GUNS & MUNITIONS CODE G301 D WILSON CODE G32 GUN SYSTEMS DIV DAHLGREN VA 22448-5000
1	CDR NSWC CODE E23 TECH LIB DAHLGREN VA 22448-5000
1	CDR NSWC ATTN CODE 3120 MR ROBERT RAST 101 STRAUS AVE INDIAN HEAD MD 20640

NO. OF COPIES	ORGANIZATION
1	CDR NSWC ATTN CODE 210P1 MR RON SIMMONS 101 STRAUS AVE INDIAN HEAD MD 20640
2	CDR NSWC ATTN CODE 6210 S BOYLES N ALMEYDA 101 STRAUS AVE INDIAN HEAD MD 20640
2	CDR NAWC ATTN CODE 3891 MR CHAN PRICE MS ALICE ATWOOD CHINA LAKE CA 93555
1	CDR NWC ATTN CODE 388 C F PRICE INFO SCIENCE DIV CHINA LAKE CA 93555-6001
1	OLAC PL TSTL ATTN D SHIPLETT EDWARDS AFB CA 93523-5000
10	CIA OFC OF CENTRAL REFERENCE DISSEMINATION BR RM GE 47 HQ WASH DC 20502
1	CIA ATTN J E BACKOFEN NHB RM 5N01 WASH DC 20505
3	DIR SNL ATTN T HITCHCOCK R WOODFIN ADV PROJ DIV 14 ORG 9123 ALBUQUERQUE NM 87185
2	DIR SNL ATTN D BENSON S KEMPKA ADV PROJ DIV 14 ORG 9123 ALBUQUERQUE NM 87185
1	DIR SNL ATTN R BEASLEY ADV PROJ DIV 14 ORG 9123 ALBUQUERQUE NM 87185

NO. OF COPIES	ORGANIZATION
2	DIR LANL ATTN B KASWHIA H DAVIS LOS ALAMOS NM 87545
1	DIR LLNL ATTN MS L355 A BUCKINGHAM PO BOX 808 LIVERMORE CA 94550
1	DIR SNL COMBUSTION RSCH FACILITY ATTN R ARMSTRONG DIV 8357 LIVERMORE CA 94551-0469
1	DIR SNL COMBUSTION RSCH FACILITY ATTN S VOSEN DIV 8357 LIVERMORE CA 94551-0469
1	DIR SNL ATTN MR MARK GRUBELICH DIV 2515 ALBUQUERQUE NM 87185
1	UNIV OF ILLINOIS DEPT OF MECH IND ENGR ATTN PROF H KRIER 144 MEB 1206 N GREEN ST URBANA IL 61801
1	JHU CPIA ATTN T CHRISTIAN 10630 LTLE PATUXENT PKWY SUITE 202 COLUMBIA MD 21044-3200
1	PENN STATE UNIV DEPT OF MECHANICAL ENGR ATTN JEFF BROWN 312 MECHANICAL ENGR BLDG UNIV PARK PA 16802
1	NCSU ATTN J G GILLIGAN BOX 7909 1110 BURLINGTON ENGR LABS RALEIGH NC 27695-7909

NO. OF COPIES	ORGANIZATION
1	NCSU ATTN M BOURHAM BOX 7909 1110 BURLINGTON ENGR LABS RALEIGH NC 27695-7909
1	STATE UNIV OF NY AT BUFFALO DEPT OF ELECTRICAL ENGR ATTN DR W J SARGEANT BONNER HALL RM 312 BUFFALO NY 14260
2	INST FOR ADVANCED TECH ATTN DR H FAIR DR T KIEHNE 4030 2 WEST BAKER LN AUSTIN TX 78759-5329
1	SPARTA ATTN DR M HOLLAND 9455 TOWNE CTR DR SAN DIEGO CA 92121-1964
2	FMC CORP ATTN MR M SEALE DR A GIOVANETTI 4800 EAST RIVER RD MINNEAPOLIS MN 55421-1498
1	FMC CORP ATTN MR J DYVIK 4800 EAST RIVER RD MINNEAPOLIS MN 55421-1498
1	HERCULES INC RADFORD ARMY AMMO PLANT ATTN D A WORRELL PO BOX 1 RADFORD VA 24141
1	HERCULES INC RADFORD ARMY AMMO PLANT ATTN E SANFORD PO BOX 1 RADFORD VA 24141
1	HERCULES INC ATTN DR R CARTWRIGHT 100 HOWARD BLVD KENVIL NJ 07847
2	OLIN ORDNANCE ATTN LIB V MCDONALD H MCELROY PO BOX 222 ST MARKS FL 32355

NO. OF COPIES	ORGANIZATION
2	OLIN ORDNANCE ATTN T BOURGEOIS D WORTHINGTON PO BOX 222 ST MARKS FL 32355
1	PAUL GOUGH ASSOC INC ATTN P S GOUGH 1048 SOUTH ST PORTSMOUTH NH 03801-5423
1	PHYSICS INTL LIB ATTN H W WAMPLER PO BOX 5010 SAN LEANDRO CA 94577-0599
1	ROCKWELL INTL ROCKETDYNE DIV ATTN BA08 J E FLANAGAN 6633 CANOGA AVE CANOGA PARK CA 91304
1	ROCKWELL INTL ROCKETDYNE DIV ATTN BA08 J GRAY 6633 CANOGA AVE CANOGA PARK CA 91304
1	PRINCETON COMBUSTION RSCH LAB ATTN N MESSINA 11 DEERPARK DR BLDG IV STE 119 MONMOUTH JCT NJ 08852
1	SCIENCE APPLICATIONS INC ATTN J BATTEH 1519 JOHNSON FERRY RD STE 300 MARIETTA GA 30062-6438
1	SCIENCE APPLICATIONS INC ATTN L THORNHILL 1519 JOHNSON FERRY RD STE 300 MARIETTA GA 30062-6438
1	ELI FREEDMAN & ASSOC ATTN E FREEDMAN 2411 DIANA RD BALTIMORE MD 21209
1	VERITAY TECHNOLOGY INC ATTN MR E FISHER 4845 MILLERSPORT HWY E AMHERST NY 14051-0305

NO. OF COPIES	ORGANIZATION
1	BATTELLE TWSTIAC 505 KING AVE COLUMBUS OH 43201-2693
1	CA INST OF TECH JET PROPULSION LAB ATTN L D STRAND MS125 224 4800 OAK GROVE DR PASADENA CA 91109
1	CA INST OF TECH JET PROPULSION LAB ATTN D ELLIOT 4800 OAK GROVE DR PASADENA CA 91109
1	GENERAL ELECTRIC CO ATTN DR J MANDZY MAIL DROP 43 220 100 PLASTICS AVE PITTSFIELD MA 01201
2	SAIC ATTN MR N SINHA DR S DASH 501 OFFICE CTR DR FT WASH PA 19034-3211
1	SAIC ATTN DR G CHRYSSAMELLIS 8400 NORMANDELE BLVD STE 939 MINNEAPOLIS MN 55437
1	IMI SERVICES USA ATTN MR G RASHBA 2 WISCONSIN CIRCL STE 420 CHEVY CHASE MD 20815

NO. OF COPIES	ORGANIZATION
	ABERDEEN PROVING GROUND
4	CDR USACSTA ATTN S WALTON G RICE D LACEY C HERUD
1	DIR USAHEL ATTN J WEISZ
35	DIR USARL ATTN AMSRL WT P ALBERT HORST AMSRL WT PC RON ANDERSON DICK BEYER JOE HEIMERL TONY KOTLAR AMSRL WT PA WILLIAM OBERLE AVI BIRK JERRY COFFEE JIM DESPIRITO DAWN GODNER ARPAD JUHASZ JOHN KNAPTON CHARLES LEVERITT MIKE MCQUAID IRVIN STOBIE PHUONG TRAN KEVIN WHITE GLORIA WREN GARY KATULKA MIGUEL DEL GUERCIO ANDY BRANT LANG MANN CHANG JOE COLBURN PAUL CONROY GEORGE KELLER DOUG KOOKER DAVE KRUCZYNSKY ROB LIEB TOM MINOR MIKE NUSCA FRED ROBBINS TODD ROSENBERGER AMSRL WT PB ED SCHMIDT AMSRL WT PD BRUCE BURNS AMSRL WT T WALTER MORRISON

NO. OF COPIES	ORGANIZATION
2	RARDE GS2 DIVISION BLDG R31 ATTN DR C WOODLEY DR G COOK FT HALSTEAD SEVENOAKS, KENT TN14 7BP ENGLAND
1	MATERIALS RESEARCH LABORATORY SALISBURY BRANCH ATTN ANNA WILDEGGER GAISSMAIER EXPLOSIVES ORDNANCE DIVISION SALISBURY SOUTH AUSTRALIA 5108
1	LABORATORIO QUIMICO CENTRAL DE ARMAMENTO ATTN CAPITAN JUAN F. HERNANDEZ TAMAYO APARTADO OFICIAL 1.105 28080-MADRID-SPAIN
1	R&D DEPARTMENT ATTN DR. PIERRE ARCHAMBAULT 5 MONTEE DES ARSENAUX LE GARDEUR, QUEBEC, CANADA J5Z 2P4
1	TZN FORSCHUNGS UND ENTWICKLUNGSZENTRUM ATTN MR T WEISE DR ING ABT SE, FACHBEREICH: HOCHLEISTUNGSPULSTECHNIK NEUENSOTHRIETHER STRAßE 20 D 3104 UNTERLUEB GERMANY
1	ERNST MACH INSTITUT ATTN DR GUSTAV ADOLF SCHROEDER HAUPTSTRAßE 18 D 7858 WEIL AM RHEIN GERMANY
2	INSTITUT FRANCO ALLEMAND ATTN DR M SAMIRANT MR D GRUNE F 68301 SAINT LOUIS CÉDEX/12 RUE DE l'INDUSTRIE, B.P. 301 FRANCE

INTENTIONALLY LEFT BLANK.

USER EVALUATION SHEET/CHANGE OF ADDRESS

This Laboratory undertakes a continuing effort to improve the quality of the reports it publishes. Your comments/answers to the items/questions below will aid us in our efforts.

1. ARL Report Number ARL-TR-692 Date of Report February 1995

2. Date Report Received _____

3. Does this report satisfy a need? (Comment on purpose, related project, or other area of interest for which the report will be used.) _____

4. Specifically, how is the report being used? (Information source, design data, procedure, source of ideas, etc.) _____

5. Has the information in this report led to any quantitative savings as far as man-hours or dollars saved, operating costs avoided, or efficiencies achieved, etc? If so, please elaborate. _____

6. General Comments. What do you think should be changed to improve future reports? (Indicate changes to organization, technical content, format, etc.) _____

CURRENT ADDRESS

Organization

Name

Street or P.O. Box No.

City, State, Zip Code

7. If indicating a Change of Address or Address Correction, please provide the Current or Correct address above and the Old or Incorrect address below.

OLD ADDRESS

Organization

Name

Street or P.O. Box No.

City, State, Zip Code

(Remove this sheet, fold as indicated, tape closed, and mail.)

(DO NOT STAPLE)